TECHNICAL REPORT BRL-TR-2890

BRL

1938 – Serving the Army for Fifty Years – 1988

SIMULATOR DIAGNOSTICS OF THE EARLY PHASE IGNITION PHENOMENA IN A 10 -MM TANK GUN CHAMBER

LANG-MANN CHANG
JOSEPH J. ROCCHIO

MARCH 1988

U.S. ARMY LABORATORY COMMAND

BALLISTIC RESEARCH LABORATORY

ABERDEEN PROVING GROUND, MARYLAND

DESTRUCTION NOTICE

Destroy this report when it is no longer needed. DO NOT return it to the originator.

Additional copies of this report may be obtained from the National Technical Information Service, U.S. Department of Commerce, Springfield, VA 22161.

The findings of this report are not to be construed as an official Department of the Army position, unless so designated by other authorized documents.

The use of trade names or manufacturers' names in this report does not constitute indorsement of any commercial product.

UNCLASSIFIED
SECURITY CLASSIFICATION OF THIS PAGE

REPORT DOCUMENTATION PAGE

Form Approved
OMB No. 0704-0188

1a. REPORT SECURITY CLASSIFICATION Unclassified	1b. RESTRICTIVE MARKINGS
2a. SECURITY CLASSIFICATION AUTHORITY	3. DISTRIBUTION/AVAILABILITY OF REPORT
2b. DECLASSIFICATION/DOWNGRADING SCHEDULE	
4. PERFORMING ORGANIZATION REPORT NUMBER(S) BRL-TR-2890	5. MONITORING ORGANIZATION REPORT NUMBER(S)
6a. NAME OF PERFORMING ORGANIZATION US Army Ballistic Research Laboratory 6b. OFFICE SYMBOL (If applicable) SLCBR-IB	7a. NAME OF MONITORING ORGANIZATION
6c. ADDRESS (City, State, and ZIP Code) Aberdeen Proving Ground Maryland 21005-5066	7b. ADDRESS (City, State, and ZIP Code)
8a. NAME OF FUNDING/SPONSORING ORGANIZATION 8b. OFFICE SYMBOL (If applicable)	9. PROCUREMENT INSTRUMENT IDENTIFICATION NUMBER
8c. ADDRESS (City, State, and ZIP Code)	10. SOURCE OF FUNDING NUMBERS PROGRAM ELEMENT NO. / PROJECT NO. 1L162618AH80 / TASK NO. / WORK UNIT ACCESSION NO.

11. TITLE (Include Security Classification)
Simulator Diagnostics of the Early Phase Ignition Phenomena in a 105-mm Tank Gun Chamber

12. PERSONAL AUTHOR(S)
Lang-Mann Chang and Joseph J. Rocchio

13a. TYPE OF REPORT	13b. TIME COVERED	14. DATE OF REPORT (Year, Month, Day)	15. PAGE COUNT
Technical Report	FROM 3/85 TO 12/85	1988 March	56

16. SUPPLEMENTARY NOTATION
Presented in part at the 8th International Symposium on Ballistics

17. COSATI CODES			18. SUBJECT TERMS (Continue on reverse if necessary and identify by block number)
FIELD	GROUP	SUB-GROUP	Gun Simulator, Ignition Studies, Ballistic Diagnostics, Pressure Data, Flamespreading, LOVA Propellant, Primer
21	02		
19	01		

19. ABSTRACT (Continue on reverse if necessary and identify by block number)

The early phase ignition phenomena in a 105-mm Tank gun chamber were investigated via diagnostics in a simulator. The study included the functioning of the ignition system, permeability of propellant bed to igniter gases, propellant bed compaction pressure wave formation, and flamespreading. Also examined were effects of the primer body configuration on ignition. The transitions found in the pressure rise and the flamespreading have been correlated with the flow change of the hot gases through the vent holes of the primer. Effects of high flow resistance in the propellant bed of small grains were seen in the recorded data. Compaction of the propellant bed could start in the very early stage of the ignition process. The addition of a vented tip to the M83 standard primer improved the uniformity of pressure distribution and flamespreading along the chamber length. The results obtained can serve as guidance for the development and assessment of new primers and interior ballistic cycle of the gun system.

20. DISTRIBUTION/AVAILABILITY OF ABSTRACT	21. ABSTRACT SECURITY CLASSIFICATION
☒ UNCLASSIFIED/UNLIMITED ☒ SAME AS RPT. ☐ DTIC USERS	Unclassified

22a. NAME OF RESPONSIBLE INDIVIDUAL	22b. TELEPHONE (Include Area Code)	22c. OFFICE SYMBOL
Lang-Mann Chang	(301) 278-6107	SLCBR-IB-P

DD Form 1472, JUN 86 Previous editions are obsolete. SECURITY CLASSIFICATION OF THIS PAGE

TABLE OF CONTENTS

TABLE OF CONTENTS (continued)

LIST OF FIGURES

TABLE OF FIGURES (CONTINUED)

TABLE OF TABLES

I. INTRODUCTION

Developments of new shaped charge (HEAT) and kinetic energy (KE) projectiles and advanced propelling charges for tank cannon ammunition have created a need for detailed diagnostics of the processes occurring during the early phase of the interior ballistic cycle. These processes include ignition, flamespreading, formation of pressure waves, and propellant bed motion and compaction. The introduction of KE or HEAT projectiles which have a complex rear section extending into the gun chamber has limited the length of the ignition system while concurrently impeding the flame spreading process. When this is coupled with the difficult to ignite low vulnerability (LOVA) propellants, the igniter-propellant bed-projectile interface system becomes critical to the optimum performance of the cartridge. To provide an adequate understanding of these processes, experimental studies have become necessary.

The present study was conducted in support of the development of the ignition system and propelling charges for the M456A2 HEAT cartridge. Although nitramine composite propellants (CAB/NC/RDX) had been designated for the cartridge, there were a variety of parameters directly affecting the ballistic performance which remained to be characterized. These parameters included the grain design, RDX particle size, primer body configuration, and igniter material. Gun firing tests would provide data to show the ballistic performance of candidate primers or charge designs, but not the detailed understanding of the phenomena occurring in the early phase of the interior ballistic cycle. In fact, this detailed information is the key basis on which advances in the right direction can be made to improve the ballistic performance. To fulfill such a need, the present work was conducted with emphasis on the functioning of the igniter, pressure wave formation, flame-spreading, and propellant bed motion.

The major apparatus for the experimental study was a 105-mm tank gun simulator. High-speed cameras, X-ray head, and pressure gages were the instrumentation used in the firing program for recording data.

II. EXPERIMENTAL APPARATUS AND PROCEDURE

Figure 1 presents a cross-sectional view of the major components of the gun simulator. The chamber of the simulator, which closely resembles the geometry and dimensions of the gun chamber, was made of a transparent cast acrylic tube with inside and outside diameters of 127 mm and 152 mm, respectively. It offers excellent transparency for the recording of the events occurring inside, see Figure 2. The chamber can withstand dynamic pressures in excess of 21 MPa (3000 psi) before rupture. Three quartz pressure gages (PCB Model 113A23) were installed, two (P_1 and P_2) at the breech and one (P_3) in the projectile tail, as indicated in the figure, for monitoring the chamber pressure. The forward end of the simulator, in which an M489 projectile (an inert training round which has the same rear configuration as the M456A2 HEAT round) was loaded, was cut from an actual gun tube. The unit was mounted on the existing fixture originally designed for the 155-mm gun simulator.

Figure 3 illustrates the experimental arrangement for the present study. In addition to the three pressure gages, the recording system includes two

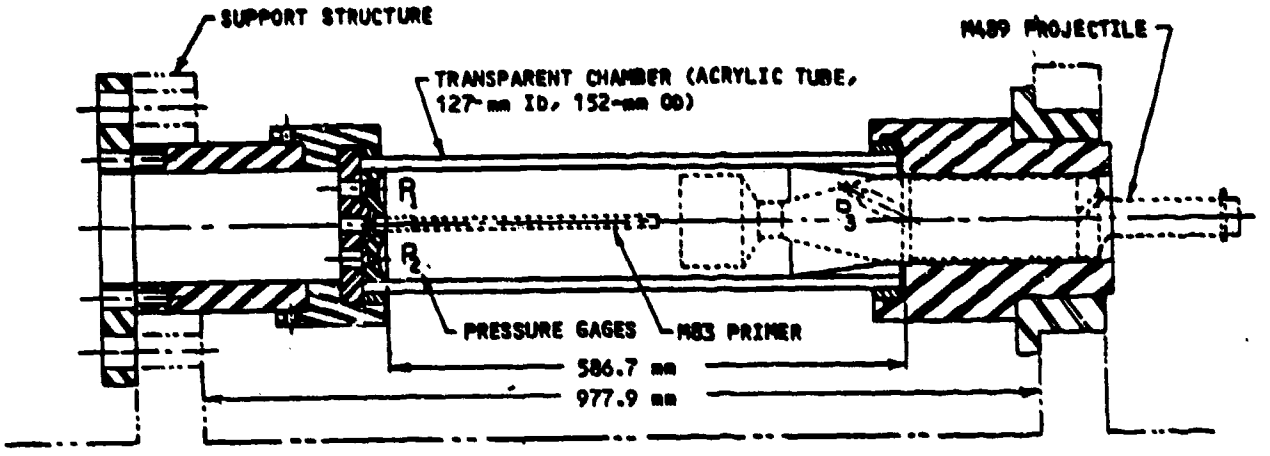

Figure 1. Cross-Sectional View of the 105-mm Gun Simulator

Figure 2. Propellant Packed Simulator Chamber

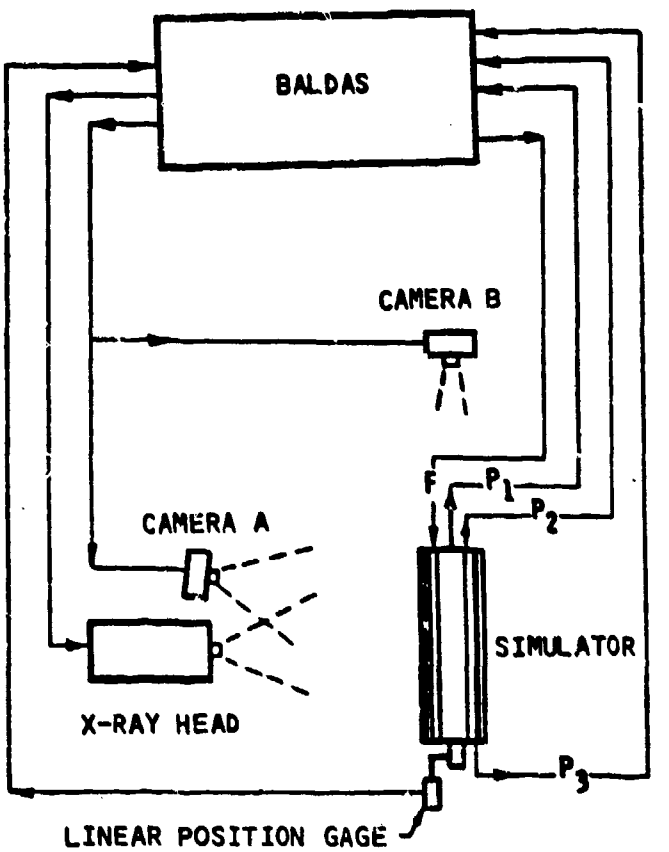

P_1, P_2, P_3: PRESSURE GAGES
F: FIRING LINE
CAMERAS: HYCAM 40, 16 mm

Figure 3. Experimental Arrangement

Hycam 40 16-mm, high-speed cameras, one X-ray head, and one linear position gage. Camera A and Camera B, located 90° apart, allow simultaneous recording of the flamespreading along the chamber length from two different angles. The camera speed was set at a framing rate of 5000 pictures per second. The flash X-ray technique has been found useful for measuring the movement of the solid phase during gun simulator firings.[1] The X-ray head was positioned on one side of the chamber and a cassette containing a Kodak XR-5 film on the opposite side to record the propellant bed motion and compaction. The linear position gage was firmly attached to the projectile nose for recording the projectile motion as a function of time. The entire fire control, data acquisition, and data reduction were performed by using the Ballistic Data Acquisition System (BALDAS) at the BRL.

The experimental study was conducted in the following sequence:

(1) Primer ignition in the open air - to observe the unperturbed functioning of the M83 standard primer.

(2) Primer ignition in an empty chamber (i.e., no propellant packed in the chamber) loaded with the M489 projectile - to investigate the venting of ignition gases from the primer and the subsequent flamespreading inside the chamber.

(3) Primer ignition in chambers packed with inert propellant grains - to observe the early development of flamespreading in the packed bed, propellent bed motion and compaction, and pressure gradient along the chamber length. In other words, the tests were to examine the functioning of the primer in the packed bed as well as the permeability of the propellant bed to igniter gases.

(4) Tests with live propelling charges - to provide insights into the early phase ignition phenomena in the interior ballistic cycle, especially the formation of pressure waves and flamespreading.

In the rounds with inert and live propellants the chambers were fully packed to minimize the presence of ullage in the chamber. The packing procedure consisted of allowing the propellant grains to freely fall into the chamber which was standing vertically.

III. RESULTS AND DISCUSSION

Prior to firing live charges, we conducted a series of experiments, including the ignition of a primer in the open air and in the chamber of the gun simulator packed with and without inert propellants. In the rounds of live charges, a variety of granular propellants, primer body configurations, and igniter materials were tested.

---

[1] Thomas C. Minor, "Characterization of Ignition Systems for Bagged Artillery Charges," ARBRL-TR-02377, USA ARRADCOM, Ballistic Research Laboratory, Aberdeen Proving Ground, MD, Oct 1981.

A. Primer Ignition in the Open Air

In this test series, three M83 standard primers (Lot LS200-70) which contained benite strands, without a vented tip, were ignited. As shown in Figure 4, the primer has 24 vent holes in the body. Two pressure gages were installed to monitor the pressure rise inside the primer tube, one near the booster end and the other near the forward end. For the recording of the event two 16-mm high-speed cameras were used, one for the side view and the other for the end view of the primer.

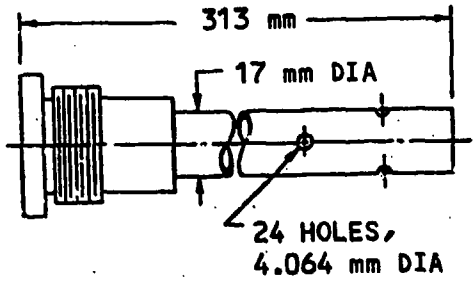

M83/STANDARD

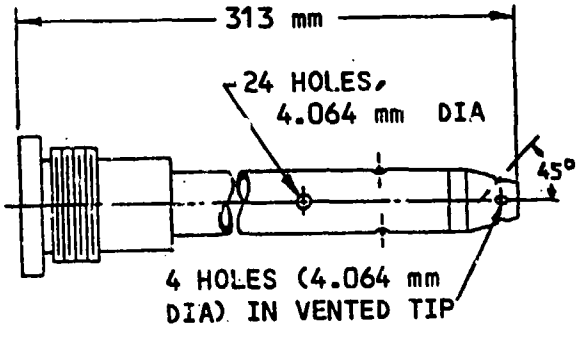

M83/E-TIP

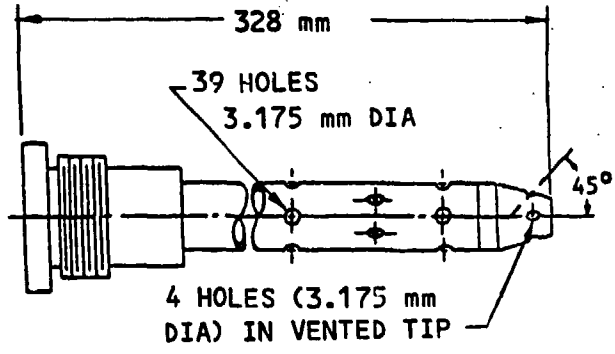

M83/EEF

Figure 4. Primer Body Configurations

1. Pressure

Figure 5 presents a set of typical pressure-time data recorded. The pressure rise near the forward end lagged 0.606 ms. Using this time interval, the average speed of the first pressure wave traveling to the forward end was calculated to be approximately 314 m/s which is close to the sound speed at one atmosphere. The two pressure curves crossed over each other for several times as the ignition process proceeded. This is believed to be due to the wave reflections at the two ends of the primer tube.

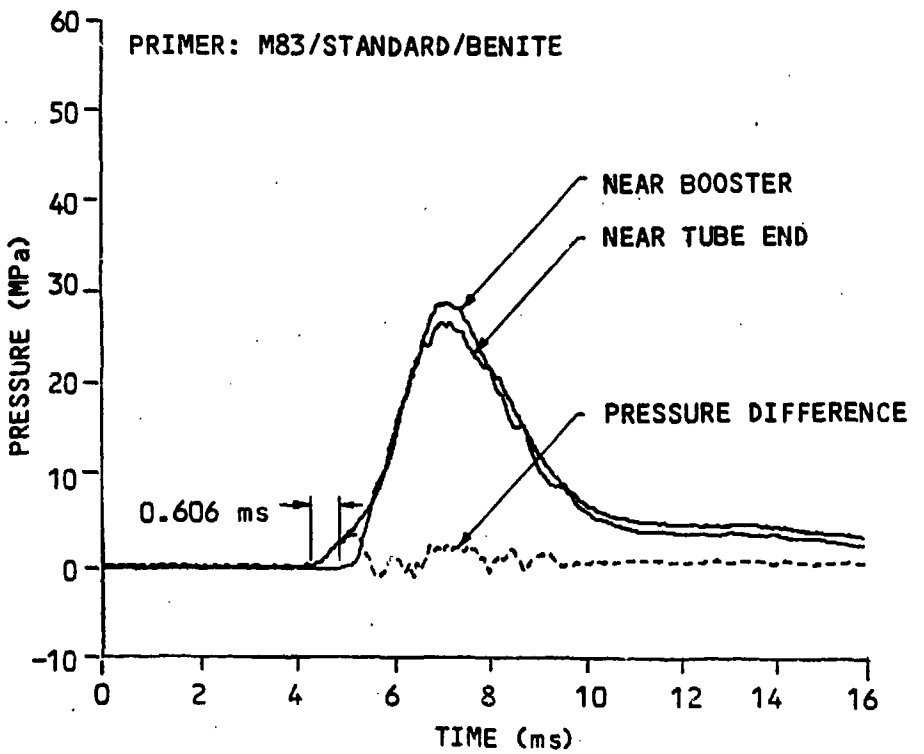

Figure 5. Pressure Recorded in an M83/Standard/Benite Primer Ignited in the Open Air

2. Flame Development

From the photographic data, the first venting of igniter gases observed located differently from one primer to another, in the range from one quarter to three quarters the primer tube length from the base. It is possible that the non-uniform lacquer coating in the individual vent holes was responsible for the variation. The time that the first venting appeared also varied, from

2.4 ms to 10 ms, or even longer, after application of the firing voltage. The venting then quickly spread over the entire length of the tube and a luminous flame was subsequently developed. The gases first vented were likely the hot gases produced by the black powder from the booster pellet rather than by the ignition of the benite strands contained in the tube.

Figure 6, printed from the high-speed film, shows an end view of the flame development around the primer. As seen in the figure, during the early development the venting was not symmetrical around the circumference of the primer tube in most of the tests. This was probably caused by a non-uniform lacquer coating and an uneven blockage of the vent holes by the benite strands inside the primer tube. Pulses of intense flame traveling away the vent holes were often seen. This may have been a result of the highly transient flow phenomenon of the venting, the non-uniformity of fuel content in the gas stream, or a sudden massive breakup of benite particles in the gas stream. The highest flame intensity was observed normally between 1 and 2 ms after the first appearance of the vented gases. The venting was sustained for more than 70 ms.

B. Primer Ignition in an Empty Chamber

The experiments with empty chambers were designed to examine the functioning of the primer, namely the flamespreading, in a confined space and to determine the pressure rise in the chamber. These data would be used as a baseline for comparisons with the data obtained subsequently from rounds packed with inert and live propellants. Three test firings were conducted using the M83 standard primer without a vented tip. Data recorded include pressures at the breech and at the projectile near the obturator as well as the flamespreading. The results obtained from these rounds were fairly reproducible.

1. Pressure

Figure 7 presents the pressures recorded at the breech and at the projectile, as indicated in Figure 1. The times in the figure are the times after the firing voltage was applied to the primer. The pressure started to rise at 4 ms and reached its maximum value, 2.6 MPa, at approximately 50 ms. There was an oscillation in a fairly regular pattern along each of the three curves from the beginning of the pressure rise. The time period between two adjacent spikes in the early segment of the curves is measured to be approximately 1.46 ms, which is close to the time (estimated to be 1.51 ms) for a sound wave to travel from one end of the chamber to the other at room temperature. The oscillation, thus, was caused by the wave reflection between the two ends of the chamber. Since the gas temperature in the chamber continued to rise and the sound speed increases with the temperature, the frequency of the oscillations along the curves thus increased as time advanced.

We note that there is a transition in the pressure curves at approximately 0.8 MPa at which the rate of the pressure rise changed considerably. Such a transition is very obvious in the case in which the chamber was packed with an inert propellant. This phenomenon will be discussed in detail in the following section (Section C).

A

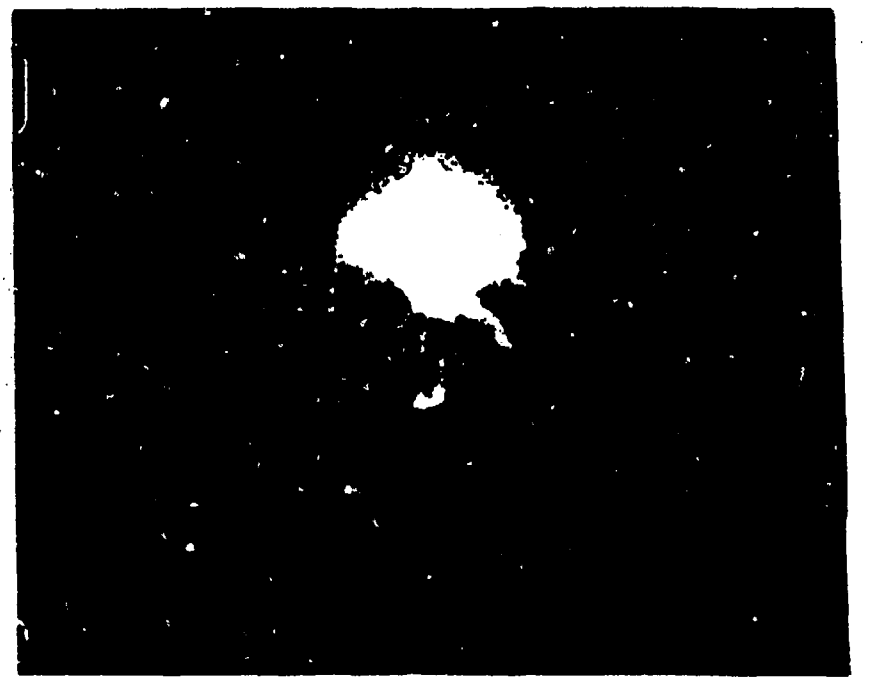

B

Figure 6. End View of the Flame Development Around an M83/ Standard/Benite Primer Ignited in the Open Air

C

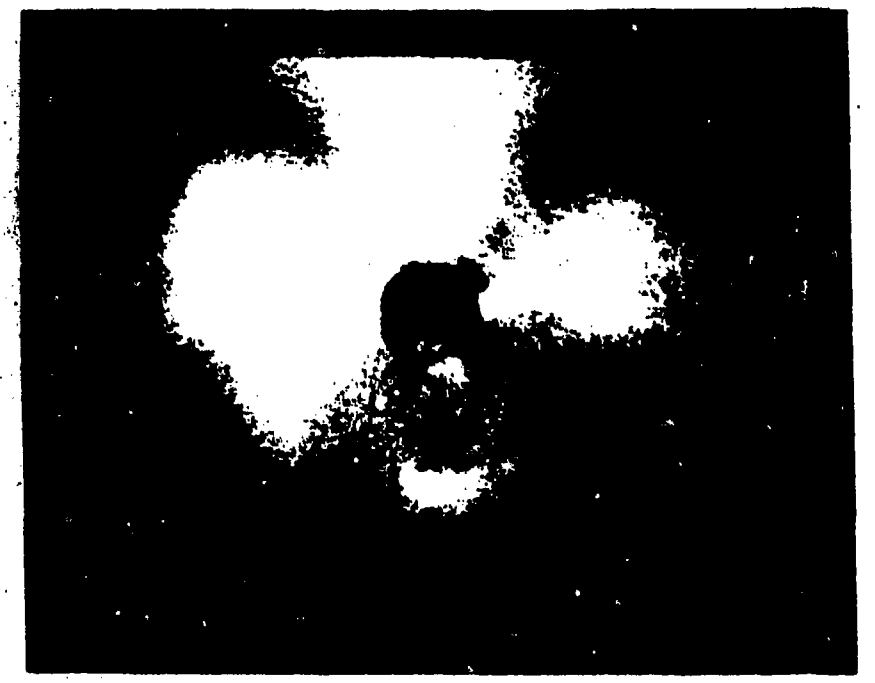

D

Figure 6. End View of the Flame Development Around an M83/ Standard/Scnite Primer Ignited in the Open Air

E

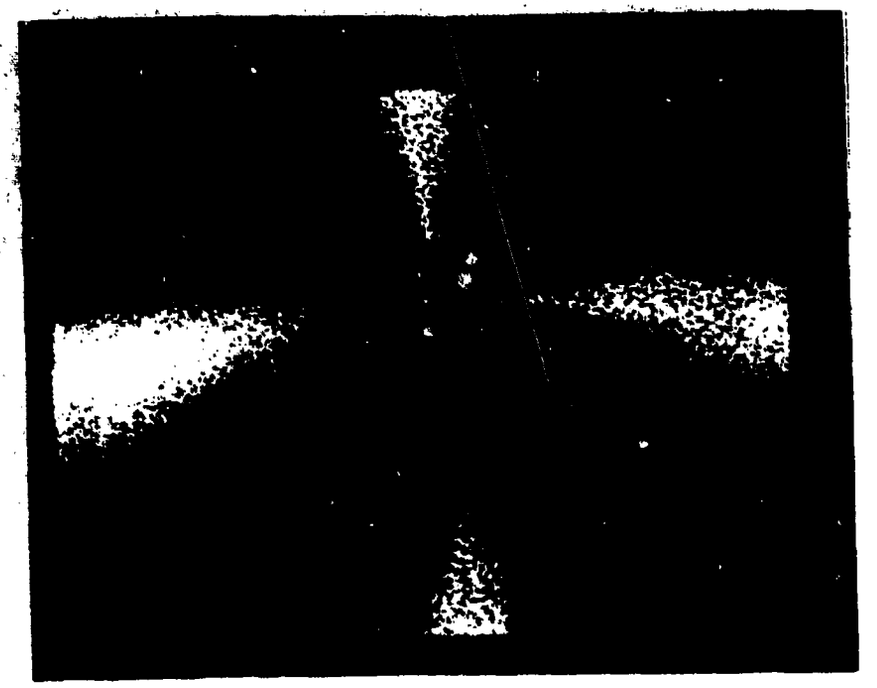

F

Figure 6. End View of the Flame Development Around an M83/ Standard/Benite Primer Ignited in the Open Air

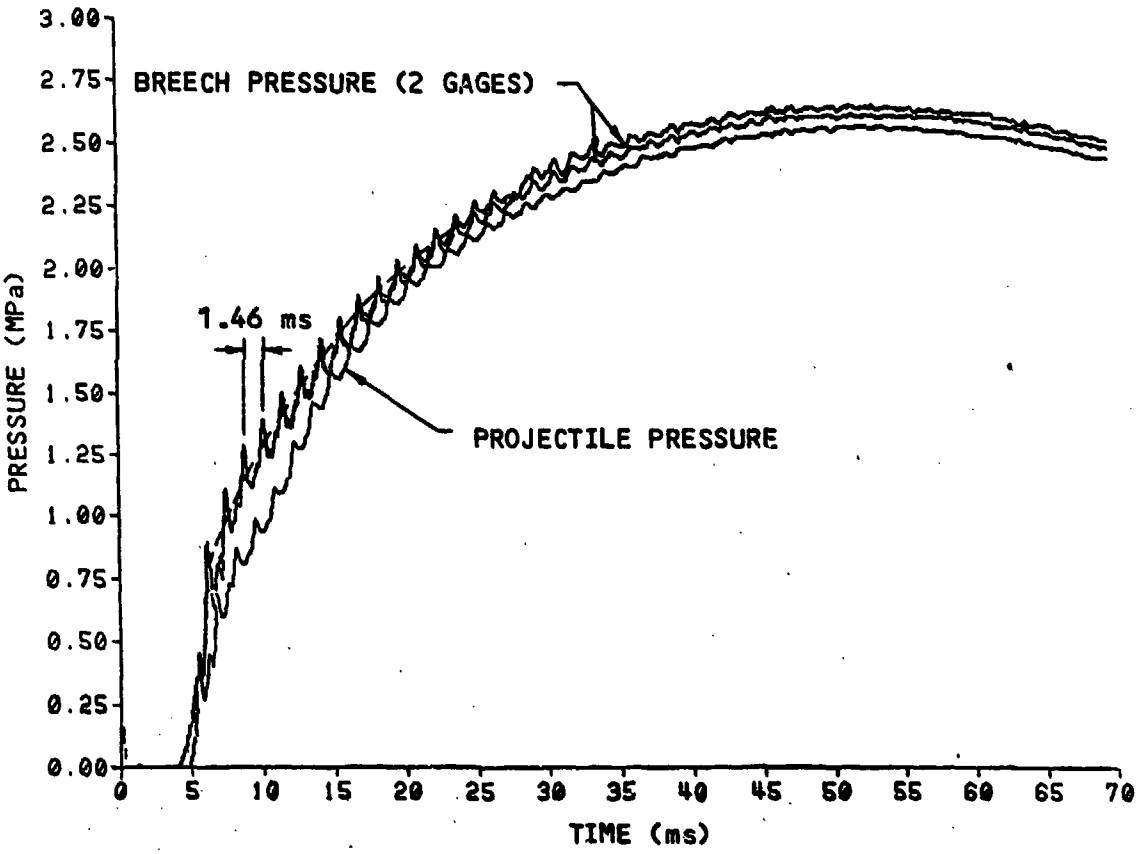

Figure 7. Pressures in an Empty Chamber

2. Flamespreading

The upper part of Figure 8 presents four frames printed from the high-speed film, showing the flame development at four given times after application of the firing voltage. The lower part of the figure is a schematic showing the sequence of flamespreading observed in the high-speed films. The first sign of gas vented from the primer was seen between the midpoint and the forward end of the primer tube at 3.5 ms. The flame then spread quickly along the tube. Jet streams developed and impinged on the chamber wall. The flame intensity reached its maximum at 4.6 ms and after that the flame started to break up into two parts, one in the breech end and the other in the projectile end. Apparently, by that time the fuel (benite) stream from the primer started fading. The jet streams carried a great amount of benite particles to the end zones of the chamber. As a result, the burning there was sustained much longer than the rest of the chamber. There is other evidence that the jet streams were carrying benite particles as we found that

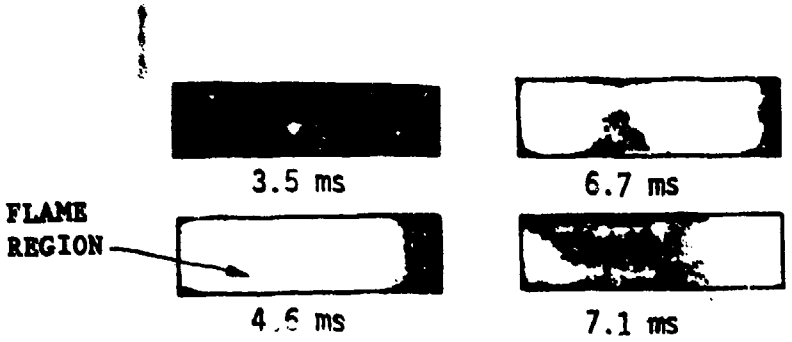

FLAME SPREADING PRINTED FROM FILM

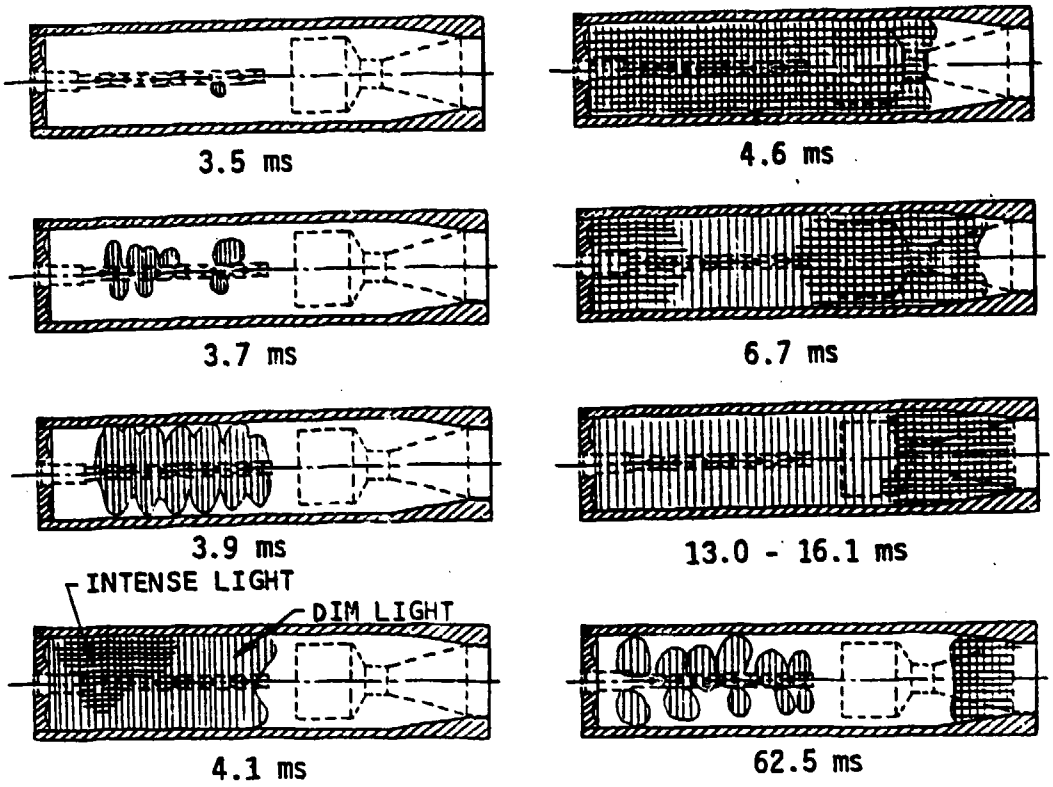

NOTE: THE TIMES INDICATED REFER TO THE TIMES
AFTER APPLICATION OF FIRING VOLTAGE

Figure 8. Flamespreading in an Empty Chamber

the chamber wall surface on which the jets directly impinged were very rough after firing. In a partially filled gun chamber, the igniter material particles transported by the gas stream may quickly reach far regions via ullage above the propellant bad. The resulting flamespreading then should be different from the case in which the chamber has no ullage. The impacts of the presence of ullage and its configuration in the chamber on the ignition process of propellant have been extensively discussed in several reports.[2-4]

C. Primer Ignition in Chambers Packed With Inert Propellants

The purpose of these tests was to characterize the propellant bed and to determine the functioning of the primer. Specifically, we examined the permeability of the propellant bed to the flow of igniter gases, the early motion of propellant grains, and the interaction between the propellant bed and the projectile.

In the present study two sizes of cylindrical grains of inert propellant were tested, 12.7 mm x 28.6 mm (diameter by length) and 5.56 mm x 6.35 mm. The large difference in grain sizes was chosen to provide a better indication of the grain size effect on bed permeability to igniter gases. Both propellants had seven perforations in each grain, but were made of different rigid plastics. The small grains were coated with graphite and thus their surfaces were more smooth. The primers used for the tests were also the M83 standard configuration loaded with benite.

1. Pressure

Figures 9 and 10 depict the pressures recorded in the chamber packed with the large grains and the small grains, respectively. The maximum breech pressures in both cases were on the order of 1.4 MPa which arrived 40 ms after application of the firing voltage. The breech pressures became level for a while after they had reached 0.8 MPa. Apparently, a transition occurred

---

[2]Thomas C. Minor, "Multidimensional Influences on Ignition, Flamespread and Pressurization in Artillery Propellant Charges," 20th JANNAF Combustion Meeting, CPIA Publication 383, Vol. I, pp. 403-414, Oct 1983.

[3]L.M. Chang and J.J. Rocchio, "Pressure-Flamespread Correlations in the Diagnostics of a Tank Gun Simulator," 1985 JANNAF Propulsion Meeting, CPIA Publication 425, Vol. III, pp. 501-516, Apr 1985.

[4]L.M. Chang, K.P. Resnik, and J.J. Rocchio, "Ignition Studies for Charge Development for an Advanced 105-mm Kinetic Energy Cartridge," 23rd JANNAF Combustion Meeting, CPIA Publication 457, Vol. II, pp. 307-317, Oct 1986.

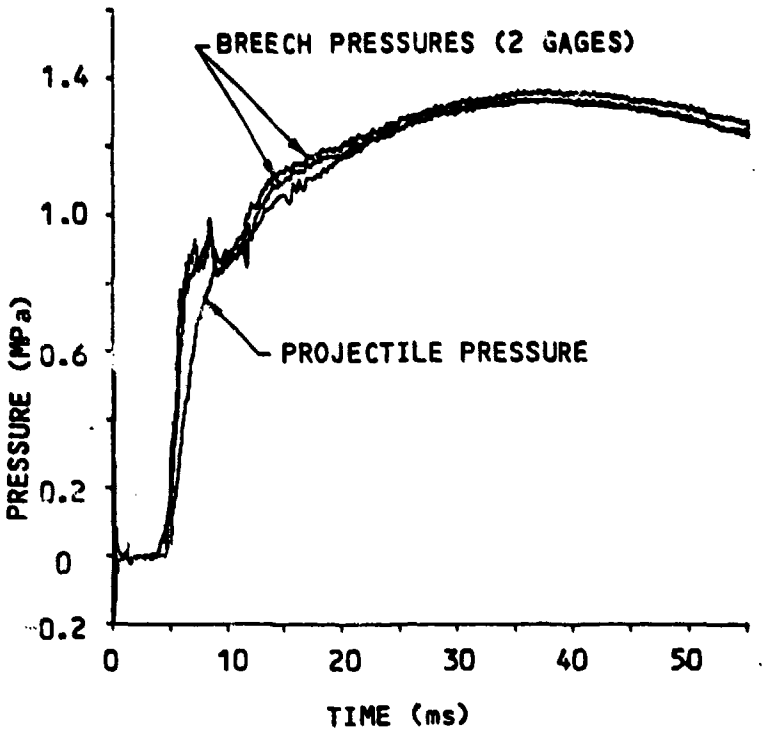

Figure 9. Pressures in an Inert Propellant Packed Chamber (Large Grains)

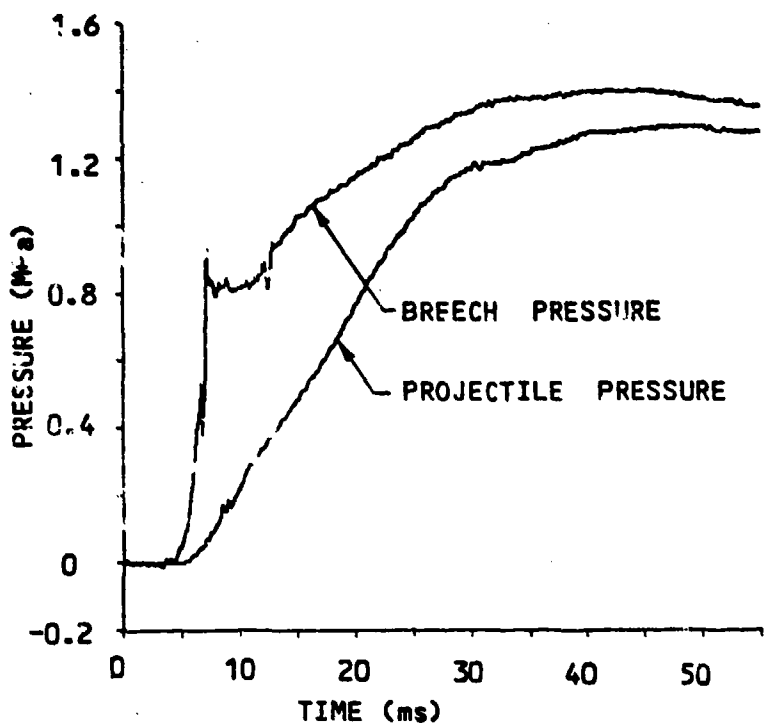

Figure 10. Pressures in an Inert Propellant Packed Chamber (Small Grains)

there as observed in the empty chamber mentioned in the previous section. The longer transition period appearing in the inert propellant packed chambers may be attributed to the effect of the heat transfer from the hot igniter gases to the inert propellant grains.

This transition is believed to have been associated with the flow change through the vent holes of the primer from choked to unchoked. From gas dynamics theory, when the pressure difference across the vent holes increases to a certain value, the gas speed through the holes reaches the limit of sound speed. After that, though the pressure difference may continuously increase, the gas speed stays at that limit. This phenomenon is called choking. The flow will return to an unchoked condition when the pressure difference becomes small enough. In the present case, the chamber pressure, denoted by P_c, initially equals atmospheric pressure. Assuming that the ratio of specific heats of the vented gases is $k = 1.2$, then the ratio of P_c to the pressure inside the primer tube, denoted by P_o, can be calculated from the following equation

$$\frac{P_c}{P_o} = [1 + M^2(k-1)/2]^{-k/(k-1)}$$

Substituting the Mach number $M = 1$ into the equation, the value of P_o at which choking occurs is 0.078 MPa (11.34 psig). Measurements of the pressure inside the M83 standard primer ignited in the open air, as the one depicted in Figure 5, show that the pressure P_o can immediately exceed 0.078 MPa and reach its peak value (typically, 40 MPa) within 1.5 to 3 ms after ignition. Thus choking occurs almost immediately following the start of the ignition of the material inside the primer. Along the pressure curve in Figure 9, the choked flow started very early and returned to an unchoked flow after the transition. Eventually, the flow speed through the vent holes gradually decreased to zero as the pressures inside and outside the primer tube approached each other.

The hole diameter is a key parameter governing the duration of the choked flow and accordingly should have a potential role in affecting the early ignition of propellant. A reduction in the hole diameter will prolong the choked flow period during which igniter gases vent at the highest rate; provided the type of charge, charge weight, and charge geometry in the primer remain the same. Figure 11 presents a typical result of breech pressure recorded in a gun firing test, showing that the breech pressure rose from 0 to 2 MPa within 1.5 ms. The propellant should have been ignited at 2 MPa since this pressure far exceeded the pressure level 1.4 MPa, shown in Figures 9 and 10, that ignition of a primer in inert propellant packed chambers was able to attain. A comparison of these two figures with Figure 11 reveals that the ignition of live propellant started around or shortly after the transition. Therefore, a longer choked flow period will achieve more effective ignition of live propellant. However, there is a limit in the reduction of hole diameter without suffering too great a reduction in gas mass flow rate to the propellant bed.

We also see that the pressure rise at the projectile afterbody lagged and was lower than the breech pressure, showing the influence of the flow resistance through the propellant bed. Direct comparisons between the breech

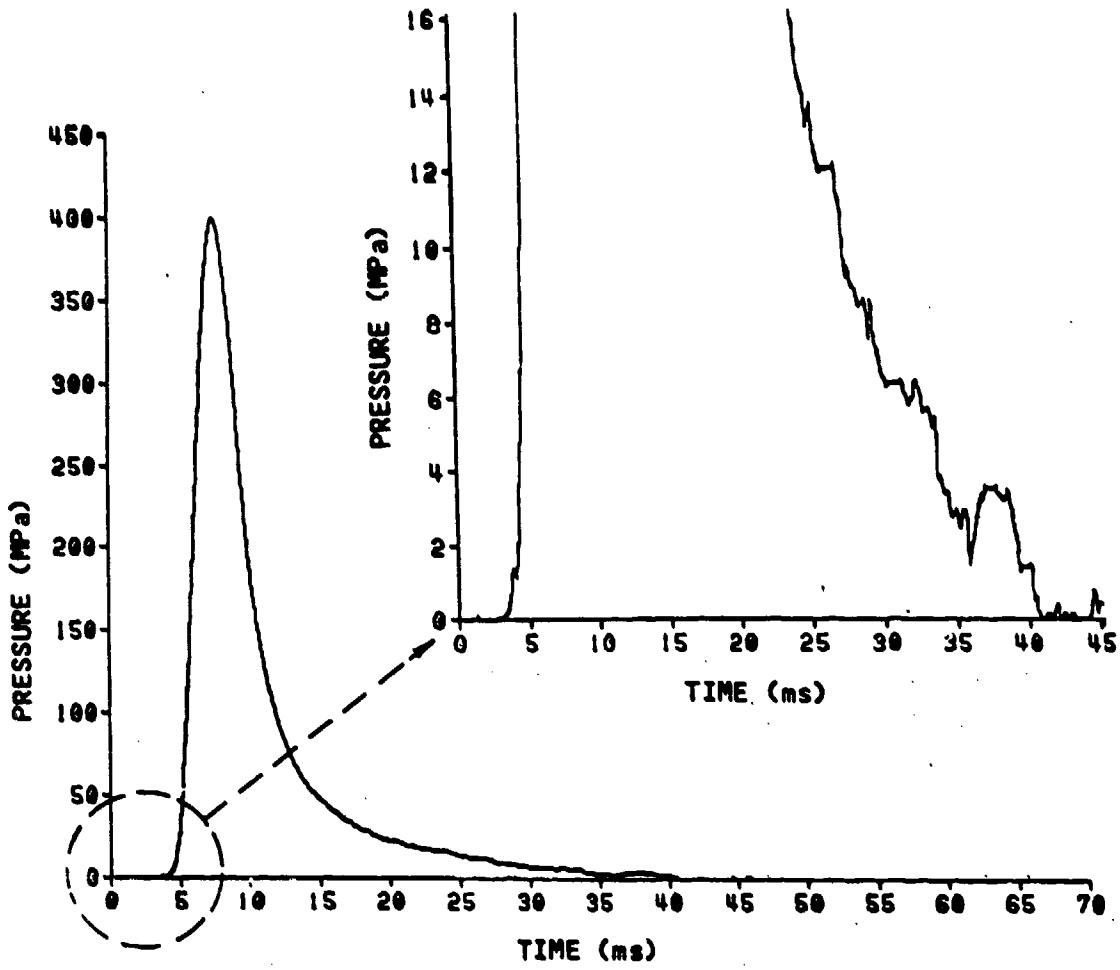

Figure 11. Typical Breech Pressure Recorded in a Gun Firing Test

pressures and between the projectile pressures for the above three chamber conditions are given in Figures 12 and 13, respectively. It is interesting to note that the pressure is higher in the empty chamber, rather than in the inert propellant packed chamber which has a smaller gas volume. This can be reasoned as a result of the heat transfer from the hot igniter gases to the grains. A quick estimate for the heat loss to the inert grains can be made as follows.

We assume that the volume occupied by the igniter gases is a thermal equilibrium system and the walls along the boundary of the system are adiabatic. We further assume that the following equation of state applies.

$$pV = CWRT \qquad (1)$$

where p = pressure
V = volume
C = compressibility factor
W = weight of gases
R = gas constant
T = temperature

Using Equation (1), we can write

$$\frac{p_e V_e}{p_i V_i} = \frac{C_e W R_e T_e}{C_i W R_i T_i} \qquad (2)$$

for the systems of the empty chamber and the system of the inert propellant packed chamber. The subscripts e and i refer to the empty chamber and the inert propellant packed chamber, respectively. Measuring from Figure 12, p_e = 2.63 MPa and p_i = 1.35 MPa after stabilization of the systems, i.e. at 50 ms. Then $p_e = 1.948\ p_i$. The gas volume of the empty chamber loaded with an M489 projectile is $V_e = 0.006145\ m^3$ (375 in^3). Assuming that the porosity of the inert propellant bed is 0.4, then $V_i = 0.4\ V_e$. The compressibility constants C_e and C_i are approximately one and are assumed to be equal. Using the Blake code, the molecular weights, M, are calculated to be 32 g/g-mole for the empty chamber and 32.2 g/mole-g for the inert propellant packed chamber, respectively. Then R_e = 0.2598 joule/gK (48.25 ft-lb/lbR) and R_i = 0.2582 joule/gK (47.95 ft-lb/lbR). After substitution into Equation (2), we obtain

$$\frac{T_e}{T_i} = 4.84 \qquad (3)$$

The gas temperature in the empty chamber can be calculated from the equation

$$T_e = \frac{p_e V_e}{W R_e} \qquad (4)$$

In the equation, the weight of the igniter gases W is 32.7 grams (0.072 pound) which is the weight of the benite strands loaded, assuming that there is no condensed phase in the systems. It is further assumed that the weight and the energy released from the M83 primer headstock is negligibly small. Substituting into Equation (4) gives

$$T_e = 1980\ K\ (3564\ R)$$

and from Equation (3), we have

$$T_i = 409\ K\ (737\ R)$$

For the heat loss calculation, we use the equation

$$\frac{Q_i}{Q_e} = \frac{W C_{vi}(T_i - T_a)}{W C_{ve}(T_e - T_a)} \qquad (5)$$

where Q_i, Q_e = heat contents in the empty chamber and the inert propellant packed chamber, respectively.

C_{vi}, C_{ve} = constant volume specific heat for the two systems, assumed to be the same.

T_a = initial temperature (ambient temperature), 294 K.

Substituting the values of T_i, T_e, and T_a into Equation (5) gives

$$\frac{Q_i}{Q_e} = 0.068$$

This result shows that only 6.8 percent of heat remained in the igniter gases in the inert propellant bed. In other words, approximately 93 percent of the heat released from the M83 primer had transferred to the inert grains up to the time that the chamber pressure became stabilized (say, 50 ms after application of the firing voltage).

Figures 12 and 13 also present an evidence of the strong influence of grain size on the pressure gradient along the chamber length. In Figure 12 the pressure curve for the small grains crosses over that for the large grains after 25 ms. It is probably because the total energy released was different from one primer to another or because a larger heat flux to the large grains in the later period of the process.

2. Propellant Bed Motion

Two flash X-rays were taken for each round, one before the firing and the other after. An overlay of the two films from the flash X-rays will

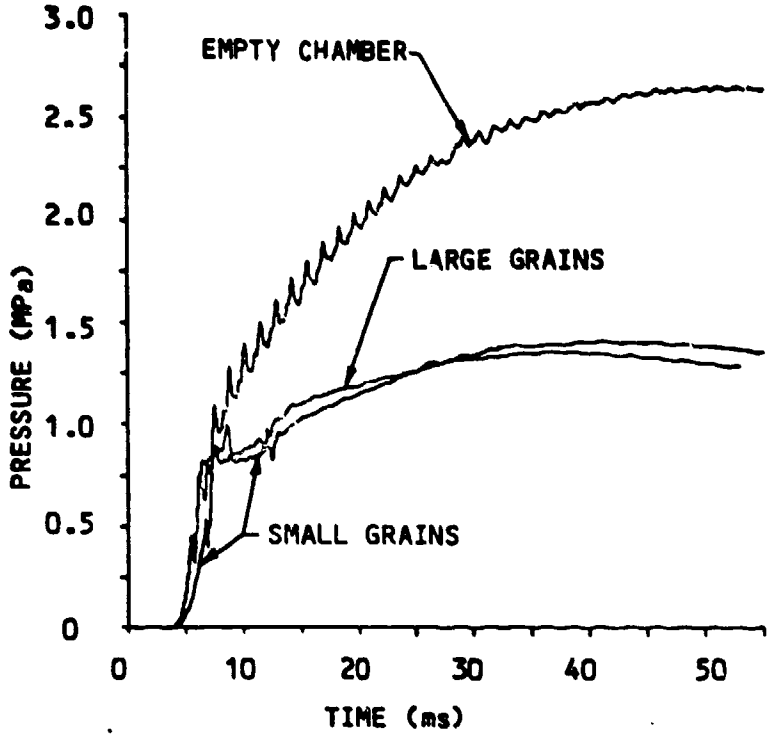

Figure 12. Breech Pressure in Empty and Inert Propellant Packed Chambers

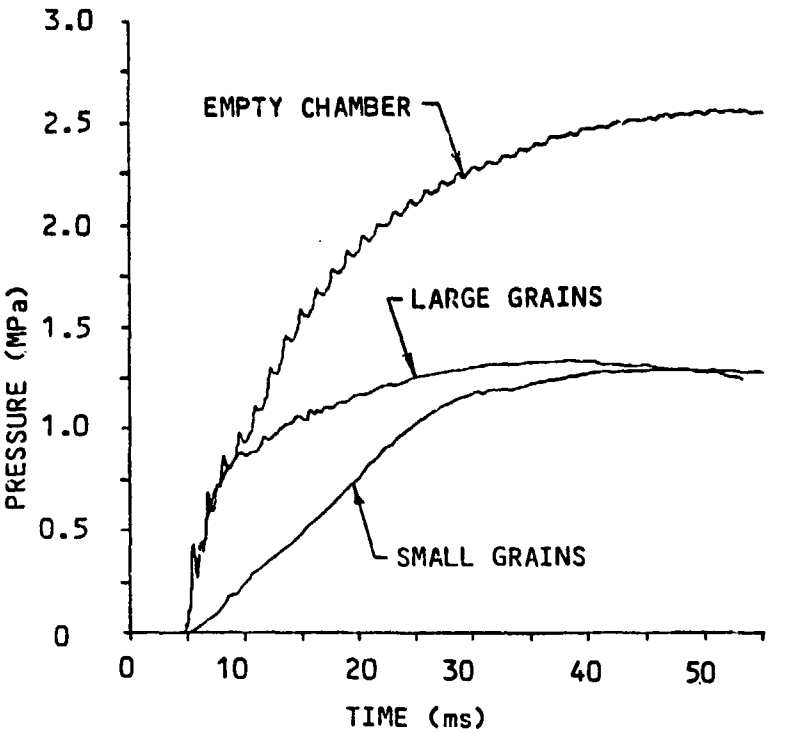

Figure 13. Projectile Pressures in Empty and Inert Propellant Packed Chambers

enable us to identify the movement of propellant grains. As seen on the X-ray films, Figure 14 shows the locations of four sample grains as well as the projectile before and after the firing. We see that grains were displaced in all directions toward the chamber walls. A small free space (ullage) which originally appeared in the upper corner of the breech end, created during the mounting of the chamber onto its fixture, no longer existed. The grains behind the projectile fin and around the cone-shaped projectile afterbody moved together with the projectile, i.e., no separation were observed at their interfaces. There was a few millimeters of projectile movement. It is unclear, however, whether such a movement resulted from the gas pressure or from the force exerted by the solid grains or both.

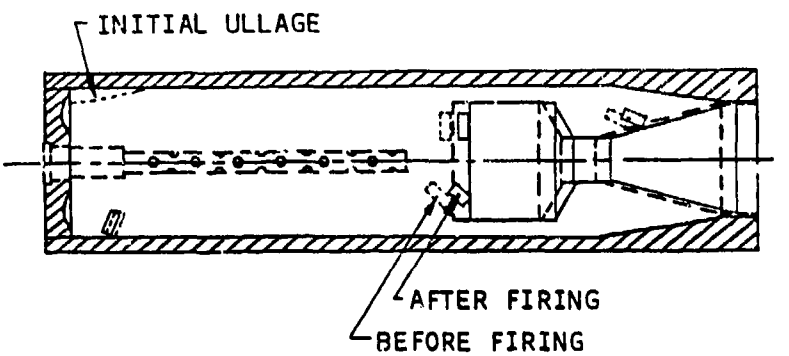

Figure 14. Inert Propellant Bed Compaction and Motion

5. Flame Pulsation

Figure 15 is a schematic of the appearance of the flame along the wall of the chamber packed with the large grains. There were two separate periods in the event. In the first period, the first light spot surfacing from the propellant bed near the midpoint of the primer section of the chamber was seen at 4 ms after the firing voltage had been applied. Subsequently, more and more light spots were seen until 5.2 ms. The light then started to diminish and the chamber turned completely dark by 12.5 ms. After a while, the flame reappeared near the breech end. The flame, again in the form of spots, quickly spread toward the front part of the chamber. The luminous area reached its maximum at 30 ms, spanning from the breech end to the projectile fin. The second period of the event was sustained for more than 70 ms. The short intermittent flame pulsation can be correlated with the transition occurring in the breech pressure.

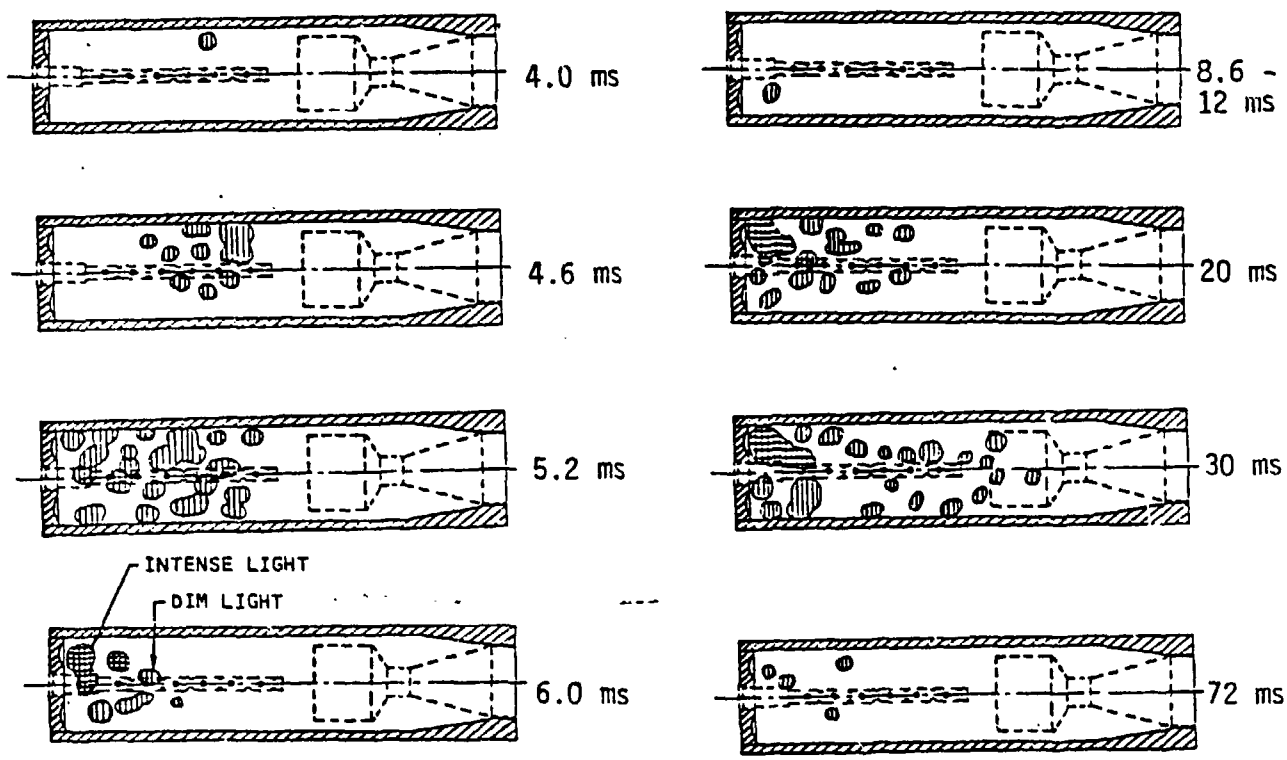

Figure 15. Flame Observed Along an Inert Propellant Packed Chamber (Large Grains)

In the rounds packed with the small grains, the light spots were rare and very dim. This provides a clear indication that a small grain propellant bed offers less permeability to igniter gases, i.e., confining the igniter gases to a smaller region.

4. Flame Intensity in the Propellant Bed

For the purpose of determining the local flame intensity (or energy deposition distribution) in the propellant bed, a number of cotton cords (3 mm in diameter and 25 mm in length) were embedded in prescribed locations inside the propellant bed, as depicted in Figure 16. The cords received various degrees of burning during firing according to their individual locations. After firing, an assembly of these cords on a plane in their original pattern

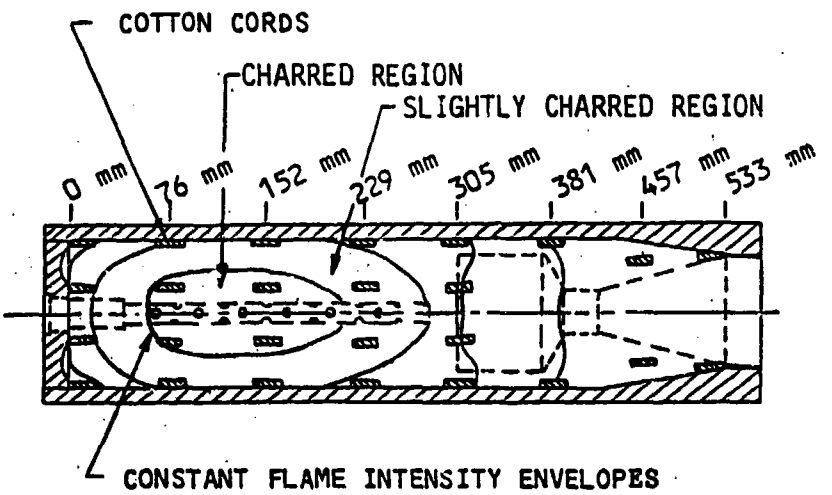

Figure 16. Flame Intensity Distribution

displayed a clear zoning of flame intensity in the propellant bed. The highest flame intensity resulting from the ignition of an M83 standard primer was found around the primer in the section between 76 mm (3 inches) and 229 mm (9 inches) from the breech end. This was in the midsection of the primer tube. The cords located near the chamber wall in that section were slightly burned. In the breech corners and in the region beyond 381 mm (15 inches), there was no sign of burning on the cords. Such a flame intensity distribution zoning shown in the figure presents another direct indication of the fact that the effectiveness of igniter gases was confined to a limited volume around the primer.

The flame intensity determined above is a result obtained at the end of the ignition process. In the case that the intensity as a function of time is needed (for instance, for the input of interior ballistics computer codes), it will require other instrumentation such as thermocouples and light intensity sensors.

D. Rounds With Live Charges

The live charges tested were M30 and four different lots of a nitramine composite propellant formulation (CAB/NC/RDX), namely lots A1-103 (7P, bimodal RDX), A2-102 (7P, unimodal RDX), A2-101 (19P, unimodal RDX), and 1289BL (7P, bimodal RDX), where P denotes perforations. The primers used had three distinct body configurations. As shown in Figure 4, they are M83/standard; M83/E-Tip (adding a vented tip to the M83/standard primer, four 4.064 mm holes in the tip); and M83/EEF (13 rows of 3 holes, each row offset 60° from the adjacent row, 4 holes in the tip, 3.175 mm in hole diameter). For comparing with benite, four candidate igniter materials for the nitramine composite propellants were tested: mixes 6828, 6779, M9+5%AL, and 6856. The composition of these materials is given in Table 1. The new materials and primer body designs were provided by the US Army Armament Research, Development, and Engineering Center in New Jersey. The tests were performed for supporting the development of new ignition systems and propelling charges for the M456A2 HEAT round.

Table 1. Composition of Candidate Igniter Materials

MIX NO.	FORMULATION	COMPOSITION (weight %)
6779	NC/NG/$KClO_4$/C/EC	55/35/8/1/1
6828	NC/NG/$KClO_4$/C/EC	26/17/57/0/1
6856	NC/KNO_3/NG/C/S/EC	35/36/15/8/5/1
M9+5%AL	NC/NG/AL/KNO_3/EC	55/38/5/1.3/0.7
Benite	NC/KNO_3/S/C/EC	39.8/44.08/6.27/9.35/0.5

The following results are presented according to the type of propellant tested, the RDX particle size used, the number of perforations in each grain, the body configuration of primer, and finally the igniter material.

1. Propellants: M30 vs. Nitramine Composites

The primers used for all of these tests belonged to the M83/standard body configuration using benite as igniter material. Figure 17 presents the pressure data recorded at the breech and the projectile for five different propellants. In the figure, t_a denotes the instant at which the breech pressure started rising, t_b the instant at which the breech pressure started rapidly rising (which was arbitrarily set at 2 MPa), t_c the instant at which the pressure reached 15 MPa (which was also arbitrarily set), and t_d the instant at which the chamber ruptured. The variability in t_a, ranging from 4.2 to 12.3 ms, largely attributed to the variations of ignition delay in the primers used. Table 2 summarizes the time data directly measured from those pressure curves. For convenience, we define the time period t_{ab} (= $t_b - t_a$) as the ignition delay of propellant, t_{ig}.

Among the nitramine composite propellants only Lot 1289BL was comparable to M30 in short ignition delay and quick pressure rise in the low pressure region. The gun firing test data given in Table 3, furnished by Deas of BRL, also have an indication that Lot 1289BL produced a higher breech pressure, P_{br}, and a larger muzzle velocity, V_{muz}, than Lot A1-103. From closed bomb tests, however, the results given in Figure 18 show that these two lots (both

are bimodal mixes with the same nominal compositions) have no significant difference in their burning rates from 27.6 MPa (4 kpsi) down to 13.8 MPa (2 kpsi). At further lower pressures over the range 1 - 4 MPa (0.15 - 0.6 kpsi), Miller and Holmes (both at BRL) used a strand burner to measure the burning rates of these two lots. Their results are listed in Table 4 which also show no significant differences in the burning rates. An explanation of the disparate behavior remains to be found.

Table 2. Time Data Measured From Figure 17

Propellants	Breech Pressure			Proj. Pressure			Proj. Disp.
	t_{ab} (ms)	t_{bc} (ms)	t_{ad} (ms)	t_{ab} (ms)	t_{bc} (ms)	t_{ad} (ms)	(mm)
M30	2.6	2.1	4.8	3.3		3.7	17.0
A1-103 (7P)	5.9	3.2	9.6	6.8	1.2	8.1	16.8
A2-102 (7P)	8.9	3.4	12.0	8.1		8.5	13.0
A2-101 (19P)	7.0	4.0	11.5	7.6	1.6	9.0	21.9
1289BL (7P)	2.4	2.5	5.5	3.1	0.6	4.1	93.7

where $t_{ab}=t_b-t_a$, $t_{bc}=t_c-t_b$, and $t_{ad}=t_d-t_a$
Primers used: M83/standard/benite

Table 3. Interior Ballistic Performance of LOVA Propellants (Lots 1289BL and A1-103) From Gun Firing Tests

Lot	Date	Temp. (C)	Charge (kg)	Projectile (kg)	P_{br} (MPa)	V_{muz} (m/s)
1289BL	6 Jun 84	21	5.216	10.505	574	1199
A1-103	6 Feb 84	20	5.715	10.120	385	1187
A1-103	6 Feb 84	20	5.715	10.092	350	1166

Table 4. Burning Rates of LOVA Propellants (Lots 1289BL and A1-103) From Strand Burner Measurements

Lot	Pressure (MPa)	Pressure (kpsi)	Burn Rates (cm/s)	Std. Dev. (cm/s)	No. of Grains
1289BL	1	0.15	0.050	+/-0.004 (8%)	4
"	2	0.30	0.082	+/-0.005 (6%)	4
"	4	0.60	0.156	+/-0.011 (7%)	4
A1-103	1	0.15	0.050	+/-0.003 (6%)	4
"	2	0.30	0.081	+/-0.005 (6%)	4
"	4	0.60	0.152	+/-0.004 (3%)	4

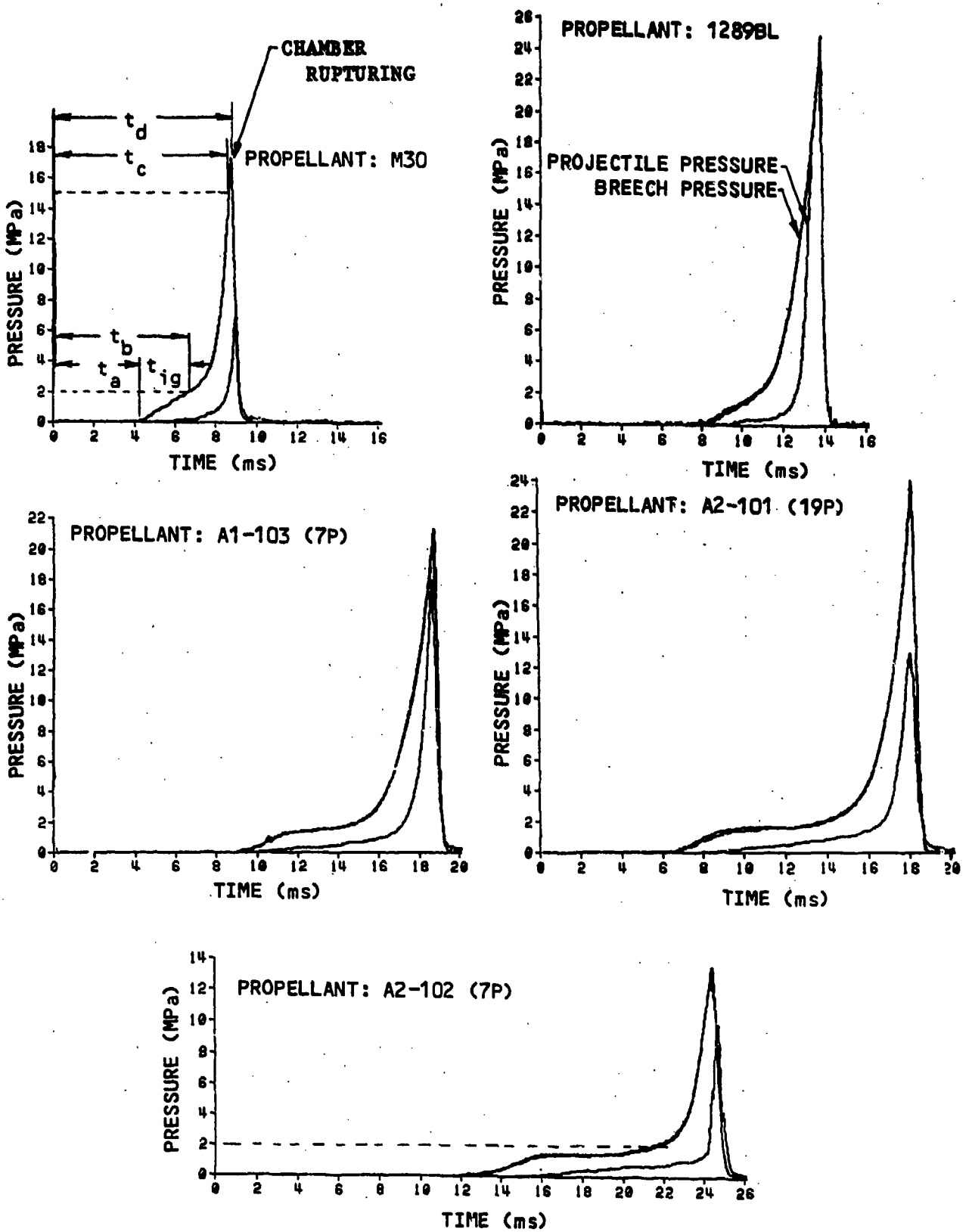

Figure 17. Pressures for M30 Propellant and LOVA Propellants (Lots 1289BL, A1-103, A2-101, and A2-102)

The breech pressure started to rise as soon as the igniter gases started venting. For Lots A1 and A2 nitramine composite propellants, the pressure then stayed almost level for a while before rising again as shown in the three sets of data in the lower part of Figure 17. During this period the pressure recorded is of the same magnitude as the pressure in the inert propellant packed chamber shown in Figure 12. Therefore, the early pressurization of the chamber before the second rise solely resulted from the ignition of the primer. We can explain that during this period the live propellant close to the primer was being heated up and then ignited. The combustion products from the propellant in this region subsequently ignited the rest of the propellant in the chamber.

The long ignition delays for A1 and A2 propellants evidence that they are difficult to ignite. This poor ignitability coupled with the complex fin assembly of the HEAT (or KE) round intruding into the gun chamber creates a strong need to optimize the ignition system in order to achieve effective ignition of the nitramine composite propellants.

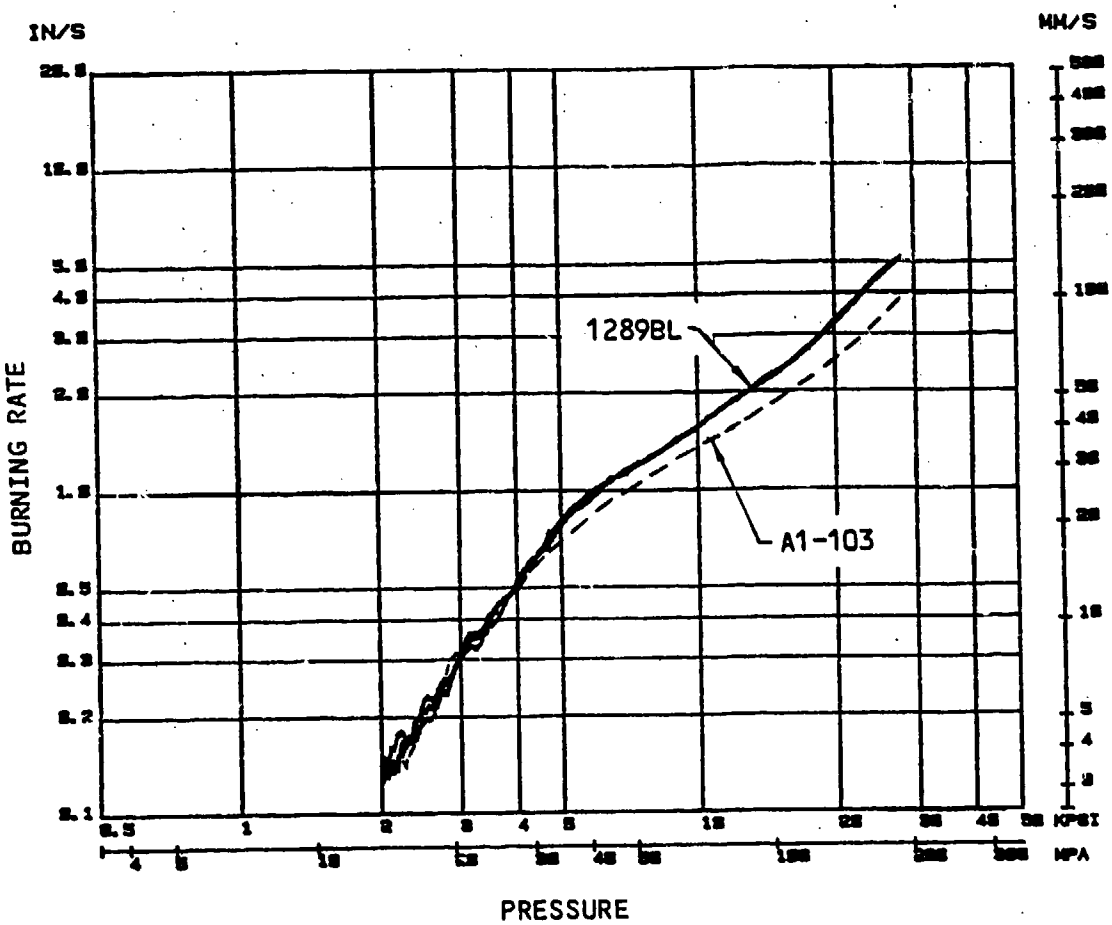

Figure 18. Burning Rates of LOVA Propellant (Lots 1289BL and A1-103) from Closed Bomb Measurements

Note that the peak values of the pressure curves shown in Figure 17 occurred immediately after the rupture of the chamber. They may vary from round to round in accordance with the material strength of the individual chamber wall and the pressurization rate in the chamber.

2. RDX Particle Sizes Used: Unimodal (A2-102) vs. Bimodal (A1-103)

Two variations of the nitramine composite formulation were studied. The difference in these materials was the RDX particle size used. The unimodal had all 5-micron weight-mean diameter RDX while the bimodal had 5-micron and 15-micron weight-mean diameter RDX in a 4:1 ratio. The unimodal propellant exhibited an overall lower burning rate and a lower pressure exponent than the bimodal formulation in closed bomb firings. A postfiring examination of samples from the simulator tests showed that only a thin film on the grain surface had burned off at the time that the chamber ruptured. It is thus more appropriate to choose propellants in close grain sizes for comparison since the grain size may present a strong effect on the early pressure rise. For this reason, we chose the bimodal propellant A1-103 to compare with the unimodal propellant A2-102. Both had about the same grain size and had the same number of perforations in each grain. The data in Table 2 show explicitly that the bimodal propellant A1-103 resulted in a shorter ignition delay and a quicker pressure rise at low pressure.

3. Primer Body Configurations: M83/Standard vs. M83/E-Tip and M83/Standard vs. M83/EEF

These three versions of the M83 primer have the same tube dimensions, but different numbers of vent holes, diameters, and arrays of the holes, see Figure 4. In the following we first compare the M83/standard with the M83/E-Tip and then with the M83/EEF.

a. M83/Standard vs. M83/E-Tip

The M83/E-Tip primer has 4 holes directed forward at 45° from the primer axis in the vented tip. These holes were designed to provide flow paths for igniter gases to quickly reach a larger region of the chamber so that more propellant can be ignited directly by igniter gases. This will reduce localization of pressure near the breech end. As expected, the pressure difference between the breech and the projectile shown in Figures 19 and 20 has been greatly reduced. However, we also note in Figure 19 that the vented tip has resulted in a longer time delay t_{ig} from the initial rise to the rapid rise of the chamber pressure. This is attributed to the addition of the vent holes in the tip which has increased the total vent area and thus shortened the duration of the high-flow-rate choked flow.

Figure 21 presents a comparison of the flamespreading observed in the high-speed film. The times listed beside the pictures are the times after application of the firing voltage and the times in the parentheses refer to the times before the chamber rupture occurred. The frame on the top in each column shows the flame first seen on the film and the frame at the bottom shows the rupturing of the chamber. An elapse of 4.6 ms from the top to the bottom frame using the M83/E-Tip primer can be compared with 2.5 ms for using the M83/standard primer. However, the flame coverage along the chamber length was larger using the M83/E-Tip primer as compared in Figure 22. The

flamespreading is consistent with the above pressure data showing that the M83/E-Tip primer has achieved a more uniform pressure distribution in the chamber.

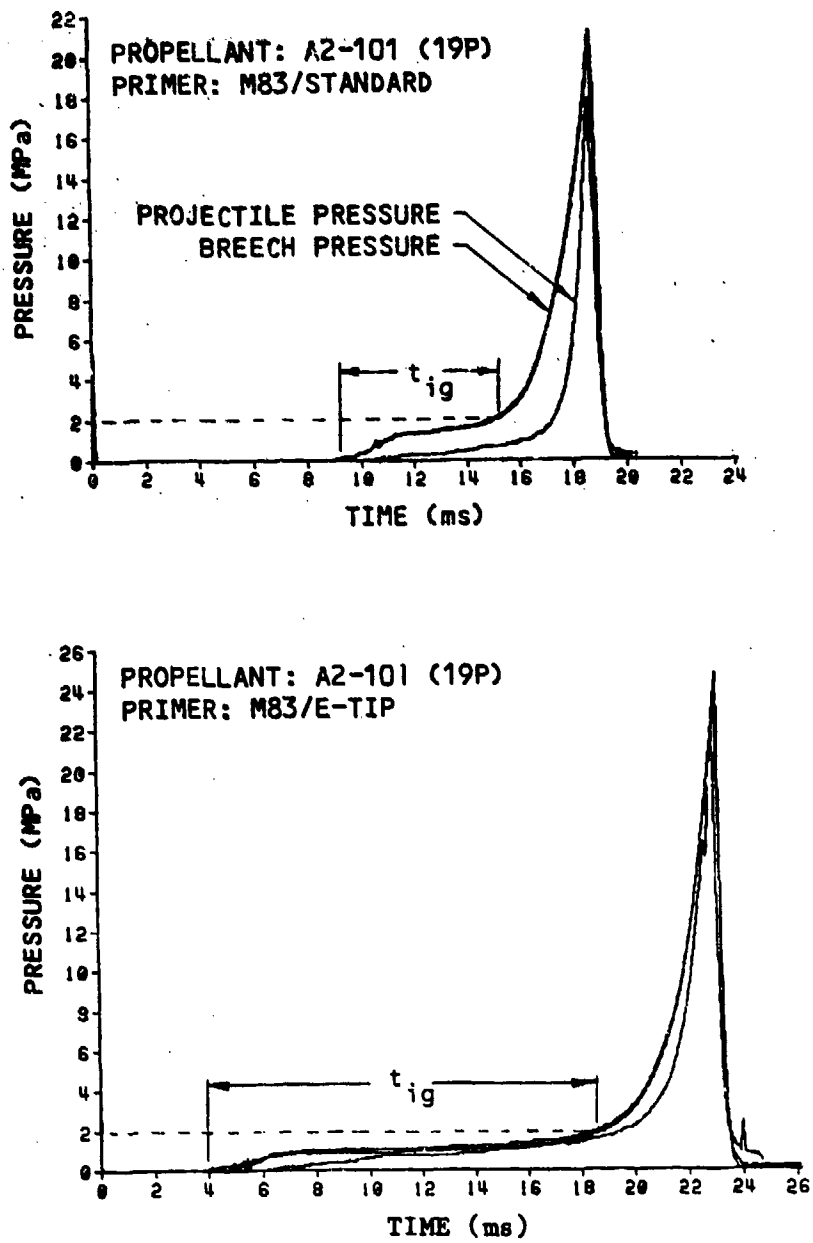

Figure 19. Pressures for A2-101 Propellant Using M83 Primers With and Without a Vented Tip

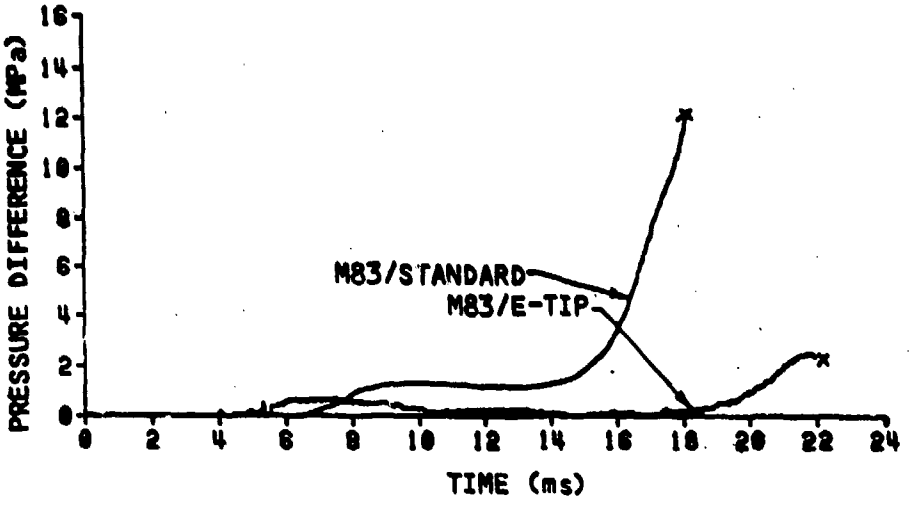

Figure 20. Pressure Difference Between Breech and Projectile for A2-101 Propellant Using M83 Primers With and Without a Vented Tip

b. M83/Standard vs. M83/EEF

As shown in Figure 4, the M83/EEF primer has 43 3.175-mm vent holes compared with 28 4.064-mm vent holes in the M83 standard primer. Due to lack of supply of A1 and A2 propellants, Lot 1289BL was used as the test propellant for evaluation of these two types of primers. Figure 23 presents two sets of pressure-time curves, one resulted from the M83 standard primer and the other from the M83/EEF primer. The figure reveals that an adoption of the M83/EEF primer has achieved a significant reduction in ignition delay. Table 5 provides a numerical comparison of their ignition delays (t_{ab} = 1.88 ms compared with 2.36 ms and t_{bc} = 1.71 ms compared with 2.49 ms). A short ignition delay is desired since the inconsistency of ballistic performance is

Table 5. Time Data Measured From Figures 23, 26, and 28

Primers	Breech Pressure					Projectile pressure					Proj Disp
	t_{ab} (ms)	t_{ac} (ms)	t_{bc} (ms)	t_{ad} (ms)	P_{max} (MPa)	t_{ab} (ms)	t_{ac} (ms)	t_{bc} (ms)	t_{ad} (ms)	P_{max} (MPa)	(mm)
St/6828	0.51	1.25	0.74	1.67	22.11	0.89	1.00	0.11	1.03	30.56	19.2
St/Benite	2.36	4.85	2.49	5.50	24.00	3.06	3.70	0.64	4.08	22.43	93.7
EEF/Benite	1.88	3.59	1.71	3.59	14.90	1.88	2.43	0.55	2.63	20.26	39.0
EEF/6828	0.35	1.01	0.66	1.31	23.50	0.27	0.32	0.05	0.44	22.24	16.0
EEF/6779	0.54	1.55	1.01	2.07	21.20	0.70	0.85	0.05	0.90	20.00	18.0
EEF/M9+5%AL	0.66	1.62	1.08	2.16	22.75	0.44	0.58	0.14	0.67	25.65	26.0
EEF/6856	0.99	2.32	1.33	2.51	21.44	1.22	1.45	0.23	1.52	17.69	26.0

where $t_{ab}=t_b-t_a$, $t_{ac}=t_c-t_a$, $t_{bc}=t_c-t_b$, $t_{ad}=t_d-t_a$, and
P_{max}= pressure at which the chamber ruptured. Propellant: Lot 1289BL.

often associated with a long ignition delay. There is also a slight improvement in the pressure difference between the breech and the projectile end as compared in the lower part of Figure 23.

A very large projectile displacement (93.7 mm, see Table 5) was measured in the round fired with the M83 standard primer. This may have resulted from a longer duration of pressure acting on the projectile and thus being accelerated for a long period.

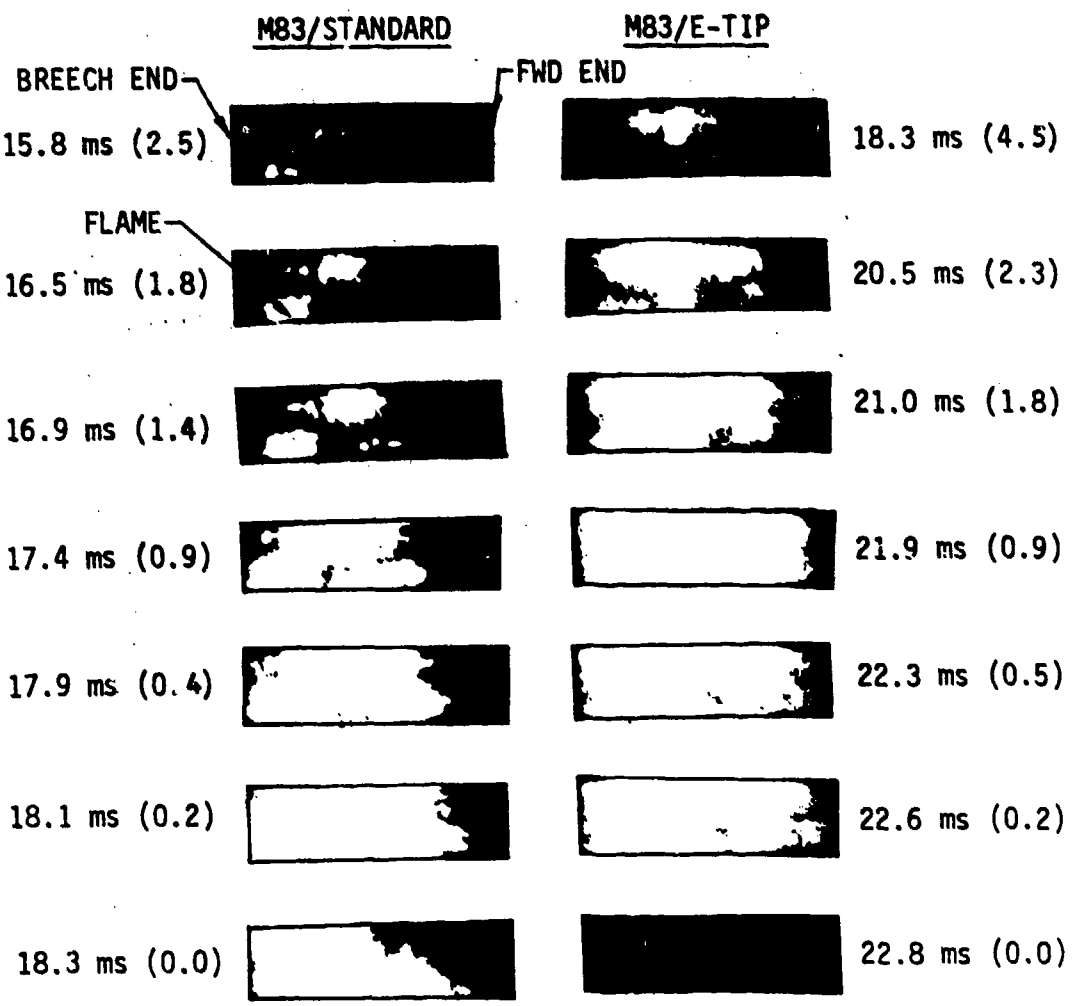

NOTE: THE TIMES INDICATED REFER TO THE TIMES AFTER APPLICATION OF FIRING VOLTAGE AND THE VALUES IN ( ) REFER TO THE TIMES BEFORE CHAMBER RUPTURE

Figure 21. Comparison of Flamespreading in Chambers With A2-101 Using M83 Primers With and Without a Vented Tip

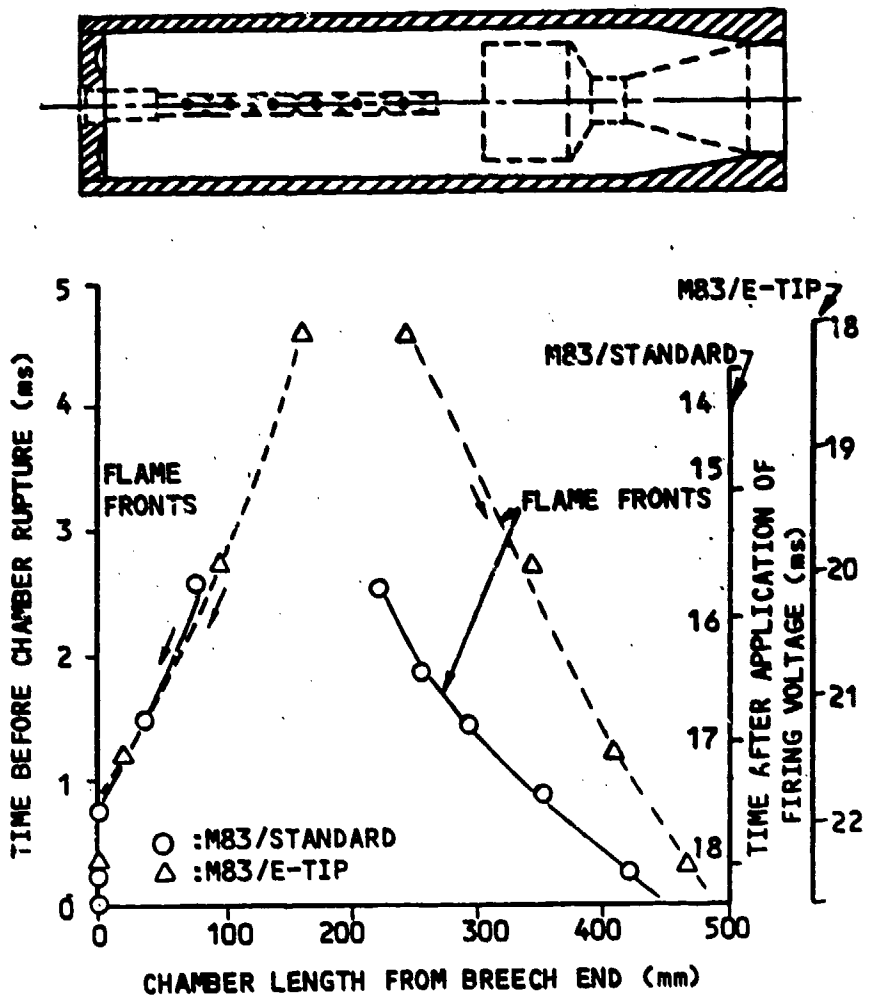

Figure 22. Flame Front Travel in Chambers With A2-101 Propellant Using M83 Primers With and Without a Vented Tip (Based on the Photographic Data in Figure 22)

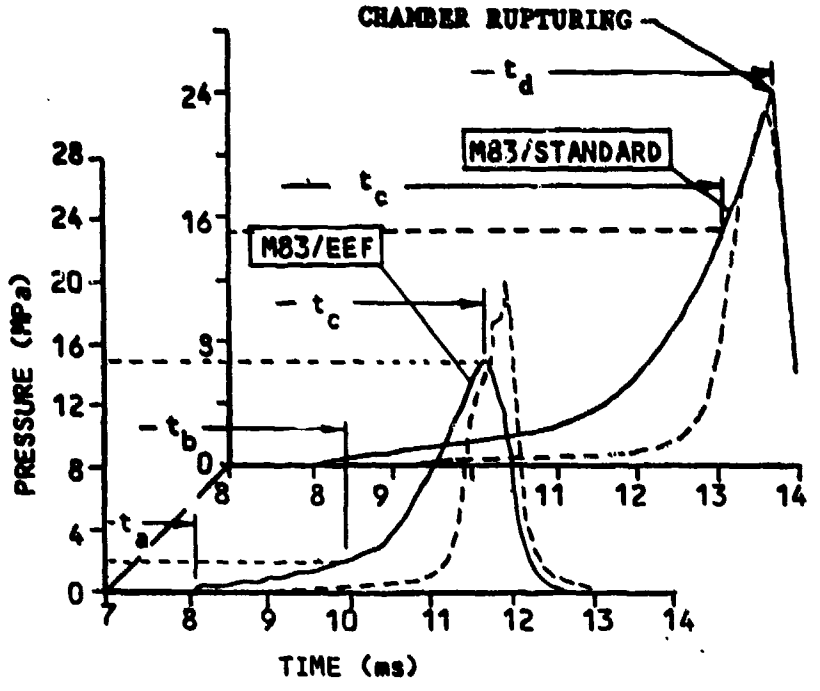

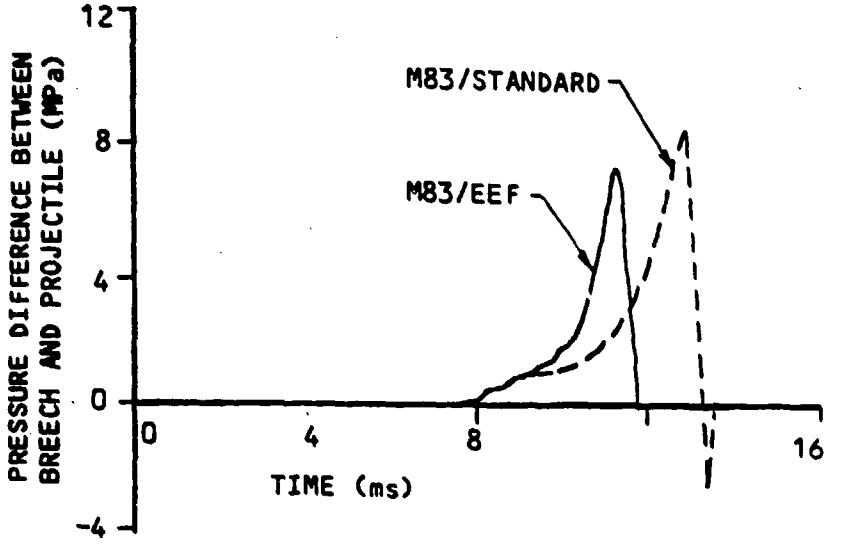

Figure 23. Pressures in Chambers Using M83/Standard and M83/EEF Primers

Figure 24 provides a comparison of flamespreading for the rounds fired using the two types of primers. The traces of their flame fronts along the chamber length as a function of time shortly before the rupture of the chamber are plotted in Figure 25. The average flame speed can be determined by examining the time needed for the flame front to travel a given distance, say the last 100 mm to the forward end of the chamber. The figure indicates that the flame needed 0.75 ms for the M83/EEF primer compared with 1 ms for the

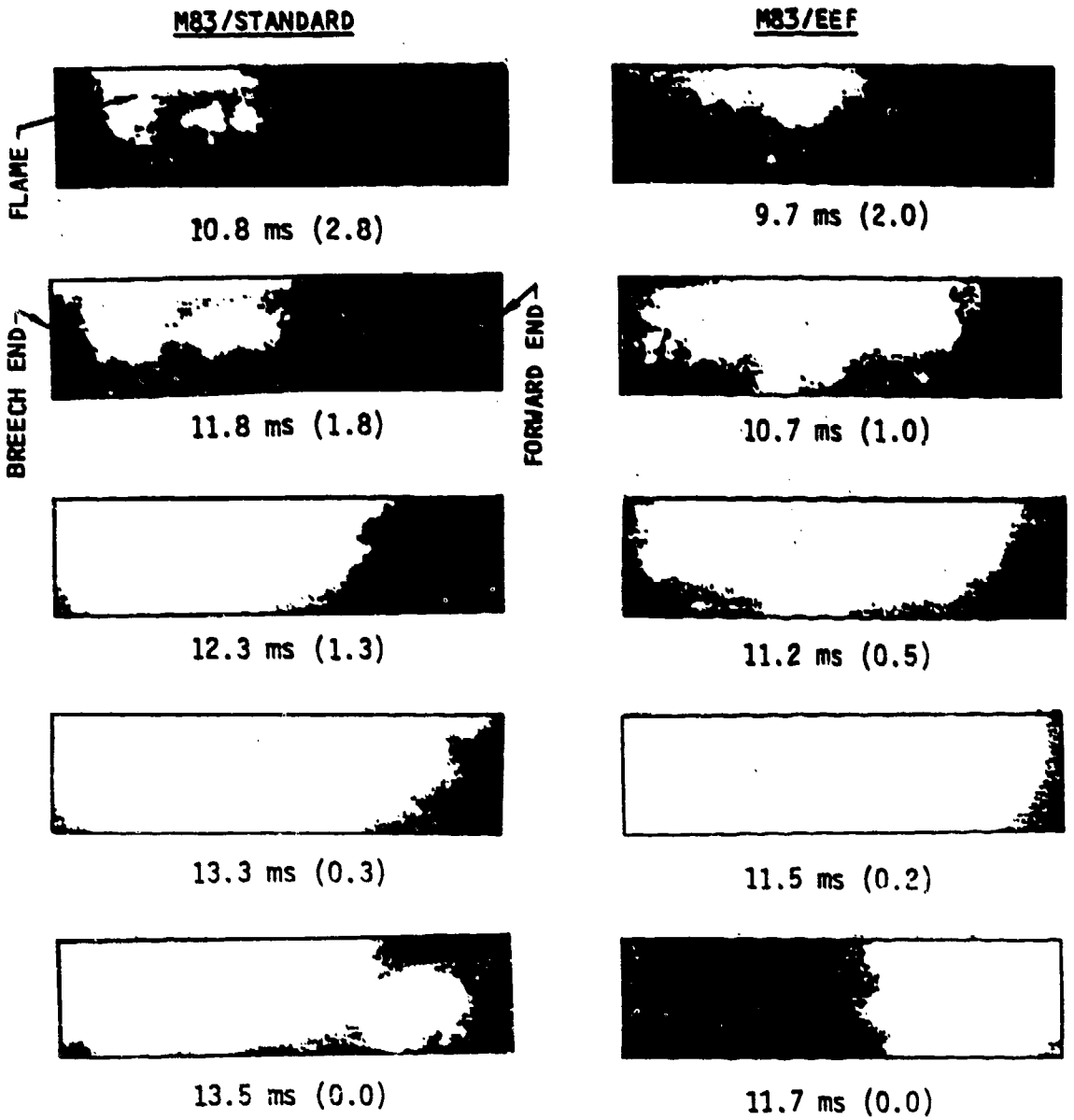

NOTE: THE TIMES INDICATED REFER TO THE TIMES AFTER APPLICATION OF FIRING VOLTAGE AND THE VALUES IN ( ) REFER TO THE TIMES BEFORE CHAMBER RUPTURE

Figure 24. Flamespreading in Chambers Using M83/Standard and M83/EEF Primers

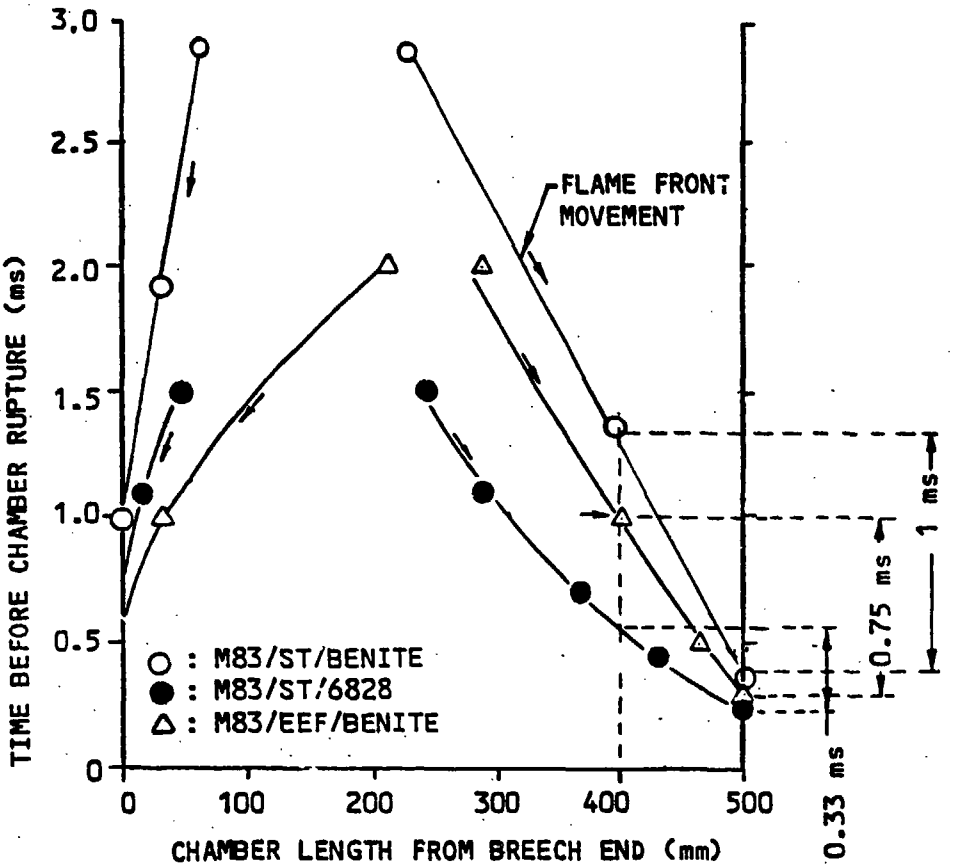

Figure 25. Flame Front Travel in Chambers Using M83/Standard/Benite, M83/Standard/6828, and M83/EEF/Benite Primers (Based on the Photographic Data in Figure 24)

standard configuration to travel that distance. This indicates that the EEF configuration has significantly improved the flamespreading along the chamber, which is in consistent with the short ignition delay discussed above. The maximum flame speed along the chamber length near the chamber end was in excess of 130 m/s.

4. Igniter Materials:

Several new igniter materials were investigated. These materials, with respect to benite, produced hotter particles, higher flame temperature, higher oxidizer content or more gaseous products. Lot 1289BL was designated as the test propellant for all of the investigations. Results obtained are presented in two groups in accordance with the type of primer used.

a. M83/Standard Primer: Benite vs. Mix 6828

Figure 26 presents the pressure-time data for the rounds fired with benite and mix 6828. The ignition delay of the round with oxygen-rich mix 6828 was substantially shorter than that with benite. However, the figure shows an adverse pressure gradient near the projectile tail (i.e., the projectile pressure overshot the breech pressure) when mix 6828 was used. It

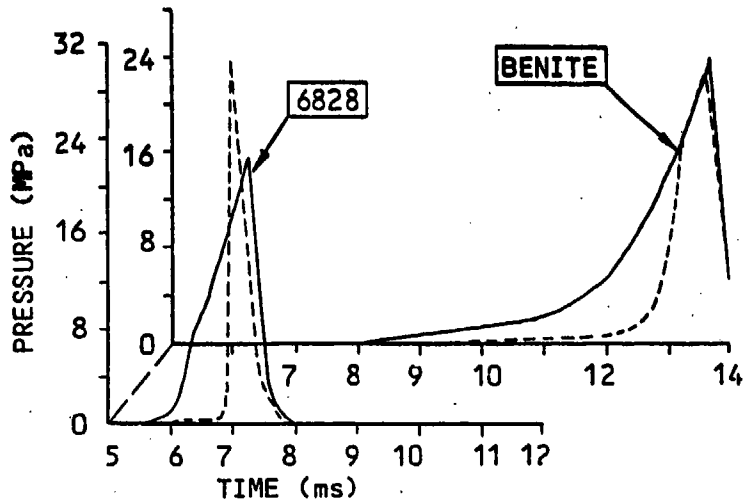

PROPELLANT: 1289BL
PRIMER: M83/STANDARD
———: BREECH PRESSURE
- - - -: PROJECTILE BASE PRESSURE

Figure 26. Pressures in Chambers Using Primers With Benite and Mix 6828

seems to be caused by vigorous ignition of propellant around the primer, which then generated a strong pressure wave, followed by flamespreading, traveling to the projectile end. Coupled with a gradual contraction of the flow path toward the forward end of the chamber and the wave reflection at the end, the pressure wave was then intensified and projectile base pressure became higher than the breech pressure. Another possibility is grain fracture occurring at the projectile base caused by a high pressurization rate in the primer section. This would increase grain burning surfaces and thus the pressure.

The flamespreading in the rounds using benite and mix 6828 is presented in Figure 27. In fact, the high-speed film clearly shows that the flame was more intense and its traveling speed along the chamber length was faster in the round using the oxygen-rich mix 6828. A comparison of their flame speeds is given in Figure 25. Again let us examine the time needed for the flame to travel the last 100 mm to the forward end of the chamber. The figure shows that it needed 0.33 ms for the round with mix 6828 compared with 1 ms with benite. The fast flamespreading correlates well with the short ignition delay indicated in the pressure data in Figure 26.

b. <u>M83/EEF Primer: Benite vs. Mixes 6828, 6779, M9+5%AL, and 6856</u>

Figure 28 displays a series of pressure data resulting from the various igniter materials. Lot 1289BL propellant and primers in the EEF configuration were used for the tests. All of these new materials exhibited a great reduction in ignition delay with respect to benite. Based on the measured data listed in Table 5, the following order can be established in accordance

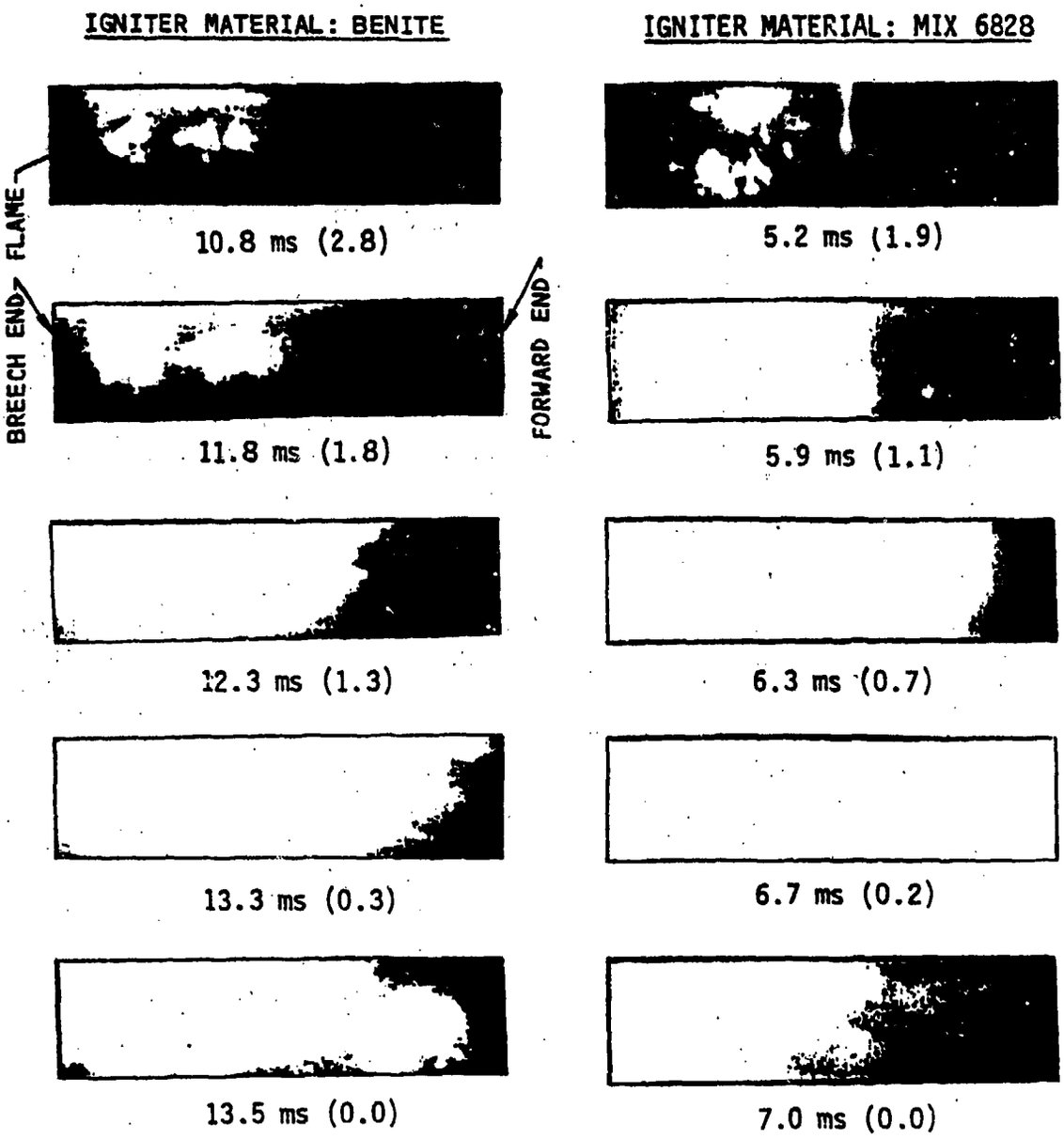

NOTE: THE TIMES INDICATED REFER TO THE TIMES AFTER APPLICATION OF FIRING VOLTAGE AND THE VALUES IN ( ) REFER TO THE TIMES BEFORE CHAMBER RUPTURE

Figure 27. Comparison of Flamespreading in Chambers Using M83/Standard/Benite and M83/Standard/6828 Primers

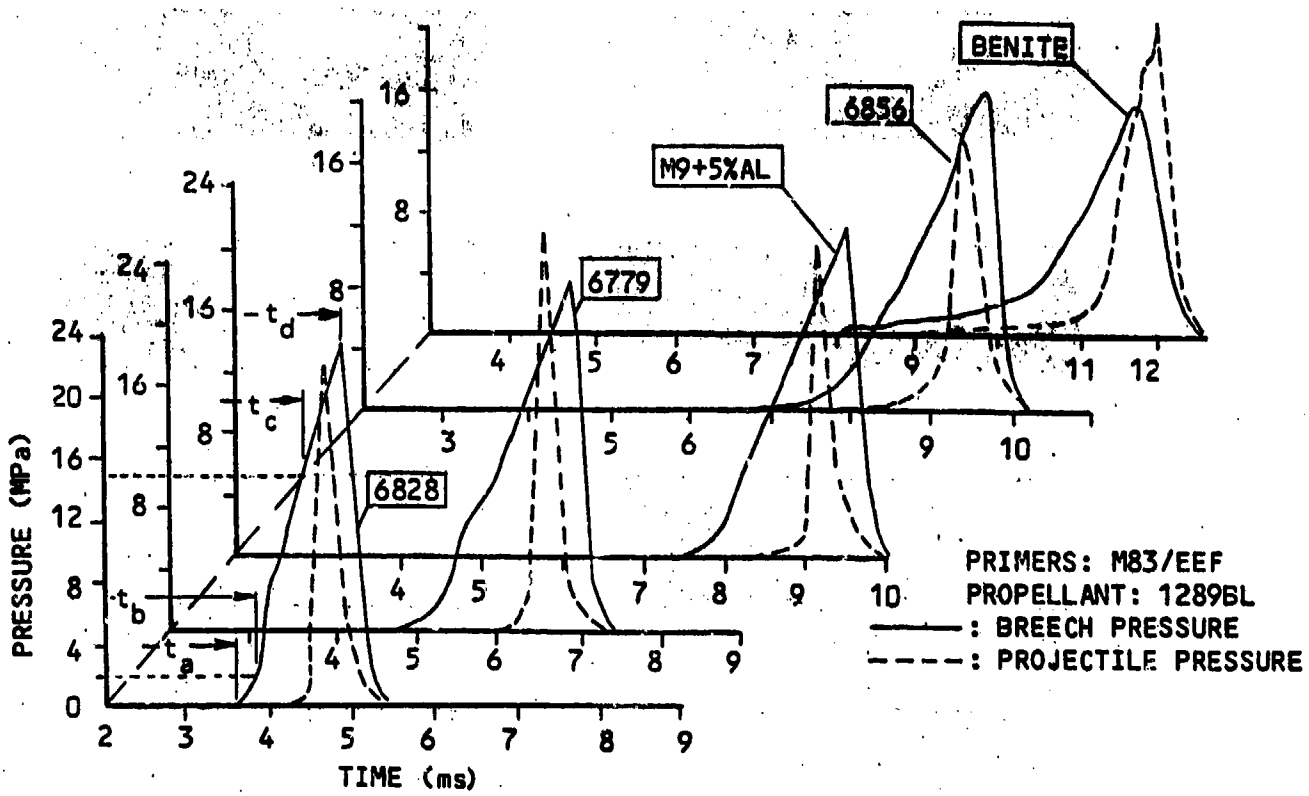

Figure 28. Pressures in Chambers Resulting From Various Igniter Materials

with the quickness with which the propellant was ignited in terms of fast pressure rise: mix 6828 > (mix 6779 and mix M9+5%AL) > mix 6856 > benite. The pressure profiles for mix 6779 and mix M9+5%AL were very similar.

The figure also shows that all of the new igniter materials resulted in an undesirable adverse pressure gradient near the forward end of the chamber. Clearly, further efforts are needed to formulate better materials which can reduce the ignition delay and also can improve the uniformity of the chamber pressure without causing an adverse pressure gradient.

5. Projectile Displacement

Figure 29 presents a typical projectile displacement which was recorded in the round fired with M30 propellant, corresponding to the pressure curves given in the upper left corner of Figure 17. The projectile started to move at 5.8 ms at which time the breech pressure had just reached 1.5 MPa and the pressure gage in the forward end had not responded yet. The projecctile continued to move for some distance after the rupture of the chamber due to the initial force.

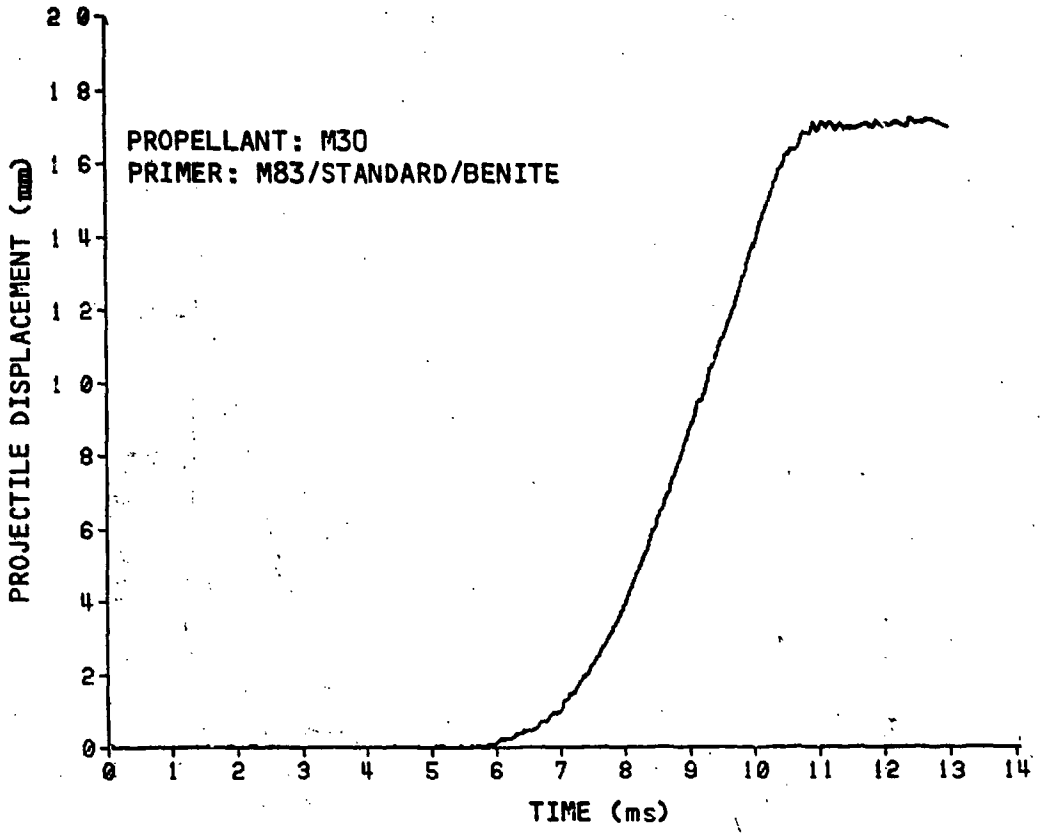

Figure 29. Typical Projectile Displacement

As we examine the data listed in Table 5, there exists a correlation between the projectile displacement and the time value t_{ad} ($= t_d - t_a$, see Figure 17 for the notations). As shown in Figure 30 the projectile displacement and thus the chamber volume increased with the increasing t_{ad}. This means that a slower pressure rise (i.e, a longer ignition delay) resulted in a larger projectile displacement before the chamber ruptured at which the breech pressure was around 20 MPa. The larger projectile displacement may have resulted from a longer duration of acceleration for the projectile.

E. Correlations of Results from Tests With the Empty Chamber, Inert Propellant Packed Chambers, and Live Charges

The transition in the pressure and flame spreading recorded in the empty and inert propellant packed chambers led to the awareness of a flow change through the primer holes, from choked to unchoked flow. The duration of the choked flow, during which the igniter gases vented at the highest rate, is believed to have a very significant effect on the ignition of propellant. This can be understood from a comparison between Figures 11 and 12. The comparison indicates that the ignition of live propellant started around or shortly after the transition. Thus, the output of a primer during the choked flow is very important. A long period of choked flow should provide more effective ignition of propellant. With the same kind of igniter material,

charge weight, and charge geometry, the duration of the choked flow is controlled by the total vent area of the primer; the smaller the total vent area, the longer the duration.

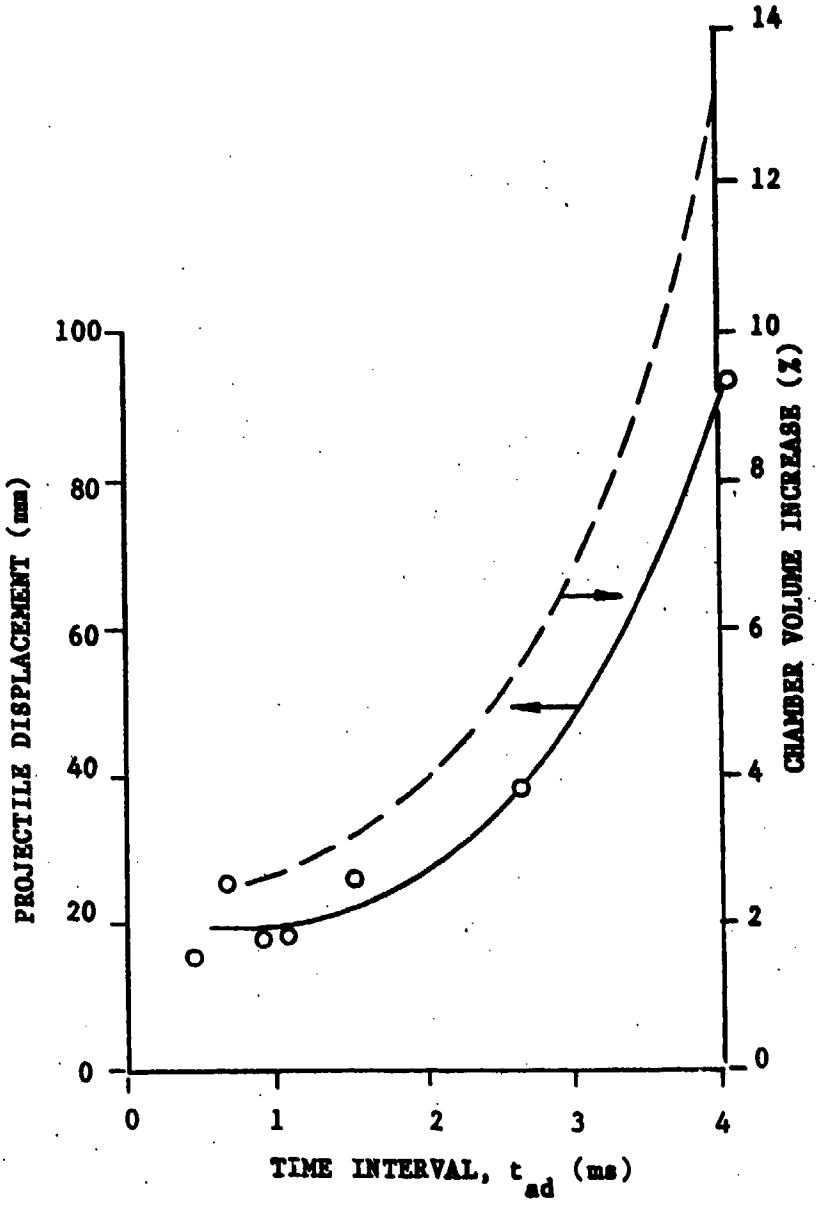

Figure 30. Projectile Displacement and Chamber Volume Increase

Results obtained from the tests with inert propellant show that there was a large pressure gradient in the propellant bed, especially in the case of small grains, see Figure 10, and the flamespreading was confined to a small region around the primer, see Figures 15 and 16. This suggests that in a live propellant bed only a limited volume of propellant close to the primer was directly ignited by the igniter gases; the combustion products of propellant in this region then ignited the rest of propellant. Thus, the number as well as the array of the vent holes becomes important to ignition. Coupled with

the discussion in the preceding paragraph, igniter body designs with more small holes but smaller total vent area and with a vented tip would allow the igniter gases to reach more propellant grains initially and would certainly achieve more effective ignition. However, there is a limit in the reduction of the total vent area without suffering too great a reduction in the gaseous mass flow rate to the propellant bed. Two new body designs with these considerations, namely the M83/E-Tip and the M83/EEF, have been tested and evidence of improved uniformity in the chamber pressure and flame spreading can be seen in Figures 20 through 26.

IV. SUMMARY AND CONCLUSIONS

This study has provided insights into the early phase ignition phenomena occurring in the 105-mm tank gun chamber. The phenomena are found to be a strong function of many variables. These include the primer body design, composition of igniter material, formulation of propellant, and configuration of propelling charge. Based on the pressure, photographic, and radiographic data obtained, the following important conclusions are presented. They can serve as guidance for the development of the advanced charges as well as for the improvement of the modeling of the interior ballistics for the tank gun system.

The test with ignition of an M83 primer in the empty simulator chamber shows that there was a significant amount of particles carried in the jet streams from the vent holes. These fuel particles sustained burning in stagnation regions for more than 10 ms. The chamber pressure exhibited apparent fluctuations as a result of the wave reflections at the two ends of the chamber.

There was a transition in the pressure rise in the inert propellant packed chamber in which an M83 primer was ignited. The transition is believed to be associated with the flow change from choked to unchoked flow through the vent holes of the primer. During the choked flow period the igniter gases vent at their maximum rate and thus a long duration of choked flow should help achieve effective ignition of nitramine composite propellants.

The result of the flame intensity measurement in the inert propellant bed indicates that the effectiveness of igniter gases was confined to regions close to the primer.

Propellant bed compaction could occur as early as the breech pressure reached 1.4 MPa. No separation was observed at the interface between the propellant bed and the cone-shaped projectile afterbody.

A comparison of the pressure data recorded in the empty chamber and the inert packed propellant chamber indicates that there was significant heat transfer from igniter gases to propellant grains following the venting process. The heat transfer could exceed 90 percent of the total heat released from the primer when the chamber pressure reached stabilization, say 50 ms after application of the firing voltage.

The data from the firings of live charges suggest that a primer with more holes in a small diameter and with a vented tip can achieve more effective

holes in a small diameter and with a vented tip can achieve more effective ignition of nitramine composite propellants. However, there is a limit in the reduction of the total vent area without suffering too great a reduction in the gaseous mass flow rate to the propellant bed.

A correlation of the pressure data obtained in the simulator tests (empty chamber, inert charges, and live charges) shows that only a limited amount of the primer efflux actually went toward propellant ignition in the rounds fired at ambient temperature.

The nitramine composite propellants tested, with the exception of Lot 1289BL, experienced a longer ignition delay and exhibited a slower initial pressure rise than M30 propellant.

The traveling speed of the flame front in a live charge could well exceed 100 m/s as it approached the forward end of the simulator chamber.

All of the oxygen-rich igniter materials tested resulted in much quicker ignition of the nitramine composite propellant than benite did. However, these materials induced an undesirable early occurrence of an adverse pressure gradient near the forward end of the simulator chamber.

ACKNOWLEDGMENTS

The authors are grateful to Dr. T. Minor and Mr. J. Evans for advice and assistance in conducting the firing program. Thanks are also due to Messrs. R. Deas, C. Ruth, and K. Resnik for their assistance in data acquisition and to Messrs. J. Bowen, J. Stabile, and J. Hewitt for instrumentation setup and firing operations.

REFERENCES

1. Thomas C. Minor, "Characterization of Ignition Systems for Bagged Artillery Charges," ARBRL-TR-02377, USA ARRADCOM, Ballistic Research Laboratory, Aberdeen Proving Ground, MD, Oct 1981.

2. Thomas C. Minor, "Multidimensional Influences on Ignition, Flamespread and Pressurization in Artillery Charges," 20th JANNAF Combustion Meeting, CPIA Publication 383, Vol. I, pp. 403-414, Oct 1983.

3. L.M. Chang and J.J. Rocchio, "Pressure-Flamespread Correlations in the Diagnostics of a Tank Gun Simulator," 1985 JANNAF Propulsion Meeting, CPIA Publication 425, Vol. III, pp. 501-516, Apr 1985.

4. L.M. Chang, K.P. Resnik, and J.J. Rocchio, "Ignition Studies for Charge Development for an Advanced Kinetic Energy Cartridge," US Army Ballistic Research Laboratory Technical Report BRL-TR-2849, Aug 1987.

DISTRIBUTION LIST

No. Of Copies	Organization
12	Administrator Defense Technical Info Center ATTN: DTIC-DDA Cameron Station Alexandria, VA 22304-6145
1	Commander USA Concepts Analysis Agency ATTN: D. Hardison 8120 Woodmont Avenue Bethesda, MD 20014-2797
1	HQDA/DAMA-ART-M Washington, DC 20310-2500
1	HQDA/DAMA-CSM Washington, DC 20310-2500
1	HQDA/SARDA Washington, DC 20310-2500
1	Commander US Army War College ATTN: Library-FF229 Carlisle Barracks, PA 17013
1	US Army Ballistic Missile Defense Systems Command Advanced Technology Center P.O. Box 1500 Huntsville, AL 35807-3801
1	Chairman DOD Explosives Safety Roard Room 856-C Hoffman Bldg. 1 2461 Eisenhower Avenue Alexandria, VA 22331-9999
1	Commander US Army Material Command ATTN: AMCPM-WF 5001 Eisenhower Avenue Alexandria, VA 22331-5001
1	Commander US Army Material Command ATTN: AMCDRA-ST 5001 Eisenhower Avenue Alexdria, VA 22331-5001
5	Project Manager Cannon Artillery Weapons System, ARDEC, AMCCOM ATTN: AMCPM-CW, F. Menke AMCPM-CWW AMCPM-CWS, M. Fisette AMCPM-CWA R. Deklaine H. Hassmann Dover, NJ 07801-5001
20	Commander US Army ARDEC, AMCCOM ATTN: SMCAR-TSS SMCAR-TDC SMCAR-LC LTC N. Barron SMCAR-AEE-BP A. Beardell D. Downs S. Einstein S. Westley S. Bernstein C. Roller J. Rutkowski SMCAR-LCB-I D. Spring SMCAR-LCE SMCAR-LCM-E S. Kaplowitz SMCAR-LCS SMCAR-CCH-T E. Barrieres R. Davitt SMCAR-LCU-CV C. Mandala SMCAR-LCW-A M. Salsbury SMCAR-AEE-BP L. Stiefel B. Brodaman Dover, NJ 07801-5001
2	Project Manager Munitions Production Base Modernization and Expansion ATTN: AMCPM-PBM, A. Siklosi AMCPM-PBM-E, L. Laibson Dover, NJ 07801-5001

DISTRIBUTION LIST

No. of Copies	Organization
3	Project Manager Tank Main Armament System ATTN: AMCPM-TMA, K. Russell AMCPM-TMA-105 AMCPM-TMA-120 Dover, NJ 07801-5001
1	Commander US Army Watervliet Arsenal ATTN: SARWV-RD, R. Thierry Watervliet, NY 12189-5001
4	Commander US Army Armament Munitions and Chemical Command ATTN: SMCAR-ESP-L Rock Island, IL 61299-7300
1	HRDA DAMA-ART-M Washington, DC 20310-2500
1	Director Benet Weapons Laboratory Armament Rech Dep & Eng Center US Army AMCCOM ATTN: SMCAR-CCB-TL Watervliet, NY 12189-5001
1	Commander US Army Aviation Research and Development Command ATTN: AMSAV-E 4300 Goodfellow Blvd. St. Louis, MO 63120-1702
1	Commander US Army TSARCOM 4300 Goodfellow Blvd. St. Louis, MO 63120-1702
1	Director US Army Air Mobility Research and Development Laboratory Ames Research Center Moffett Field, CA 94035-1099
1	Commander US Army Communications - Electronics Command ATTN: AMSEL-ED Fort Monmouth, NJ 07703-5301
1	Commander ERADCOM Technical Library ATTN: DELSD-L (Report Section Fort Monmouth, NJ 07703-5301
1	Commander US Army Harry Diamond Lab. ATTN: DELHD-TA-L 2800 Powder Mill Road Adelphi, MD 20783-1145
1	Commander US Army Missile Command ATTN: AMSMI-CM Redstone Arsenal, AL 35898-5249
1	Director US Army Missile and Space Intelligence Center ATTN: AIAMS-YDL Redstone Arsenal, AL 35898-5500
1	Commander US Army Missile Command Research, Development, and Engineering Center ATTN: AMSMI-RD Redstone Arsenal, AL 35898-5500
1	Commander US Army Aviation School ATTN: Aviation Agency Fort Rucker, AL 36360
1	Commander US Army Tank Automotive Command ATTN: AMSTA-TSL Warren, MI 48092-2498

DISTRIBUTION LIST

No. of Copies	Organization
1	Commander US Army Tank Automotive Command ATTN: AMSTA-CG Warren, MI 48092-2498
1	Project Manager Improved TOW Vehicle ATTN: AMCPM-ITV US Army Tank Automotive Command Warren, MI 48092-2498
2	Project Manager M1 Abrams Tank Syatems ATTN: AMCPM-GMC-SA, T. Dean Warren, MI 48092-2498
1	Project Manager Fighting Vehicle Systems ATTN: AMCPM-FVS Warren, MI 48092-2498
1	President US Army Armor & Engineer Board ATTN: ATZK-AD-S Fort Knox, KY 40121-5200
1	Project Manager M-60 Tank Development ATTN: AMCPM-M60TD Warren, MI 48092-2498
1	Director US Army TRADOC Systems Analysis Activity ATTN: ATAA-SL White Sands Missile Range, NM 88002
1	Commander US Army Training & Doctrine Command ATTN: ATCD-MA/ MAJ Williams Fort Monroe, VA 23651
2	Commander US Army Materials and Mechanics Research Center ATTN: AMXMR-ATL Tech Library Watertown, MA 02172
1	Commander US Army Research Office ATTN: Tech Library P.O. Box 12211 Research Triangle Park, NC 27709-2211
1	Commander US Army Belvoir Research & Development Center ATTN: STRBE-WC Fort Belvoir, VA 22060-5606
1	Commander US Army Logistics Mgmt Ctr Defense Logistics Studies Fort Lee, VA 23801
1	Commander US Army Infantry School ATTN: ATSH-CD-CSO-OR Fort Benning, GA 31905
1	President US Army Artillery Board Ft. Sill, OK 73503-5600
1	Commandant US Army Command and General Staff College Fort Leavenworth, KS 66027
1	Commandant US Army Special Warfare School ATTN: Rev & Tng Lit Div Fort Bragg, NC 28307
3	Commander Radford Army Ammunition Plant ATTN: SMCRA-QA/HI LIB Radford, VA 24141-0298

DISTRIBUTION LIST

No. of Copies	Organization
1	Commander US Army Foreign Science & Technology Center ATTN: AMXST-MC-3 220 Seventh Street, NE Charlottesville, VA 22901-5396
2	Commandant US Army Field Artillery Center & School ATTN: ATSF-CO-MW, B. Willis Ft. Sill, OK 73503-5600
1	Commander US Army Development and Employment Agency ATTN: MODE-TED-SAB Fort Lewis, WA 98433-5099
1	Chief of Naval Material Department of Navy ATTN: J. Amlie Arlington, VA 20360
1	Office of Naval Research ATTN: Code 473, R. S. Miller 800 N. Quincy Street Arlington, VA 22217-9999
3	Commandant US Army Armor School ATTN: ATZK-CD-MS M. Falkovitch Armor Agency Fort Knox, KY 40121-5215
2	Commander Naval Sea Systems Command ATTN: SEA 62R SEA 64 Washington, DC 20362-5101
1	Commander Naval Air Systems Command ATTN: AIR-954-Tech Lib Washington, DC 20360
1	Assistant Secretary of the Navy (R, E, and S) ATTN: R. Reichenbach Room 5E787 Pentagon Bldg. Washington, DC 20350
1	Naval Research Lab Tech Library Washington, DC 20375
5	Commander Naval Surface Weapons Center ATTN: Code G33, J. L. East W. Burrell J. Johndrow Code G23, D. McClure Code DX-21 Tech Lib Dahlgren, VA 22448-5000
2	Commander US Naval Surface Weapons Center ATTN: J. P. Consaga C. Gotzmer Indian Head, MD 20640-5000
4	Commander US Naval Surface Weapons Center ATTN: S. Jacobs/Code 240 Code 730 K. Kim/Code R-13 R. Bernecker Silver Springs, MD 20903-5000
2	Commanding Officer Naval Underwater Systems Center Energy Conversion Dept. ATTN: Code 5B331, R. S. Lazar Tech Lib Newport, RI 02840

DISTRIBUTION LIST

No. of Copies	Organization
4	Commander Naval Weapons Center ATTN: Code 388, R. L. Derr C. F. Price T. Boggs Info. Sci. Div. China Lake, CA 93555-6001
2	Superintendent Naval Postgraduate School Department of Mechanical Engineering Monterey, CA 93943-5100
1	Program Manager AFOSR Directorate of Aerospace Sciences ATTN: L. H. Caveny Bolling AFB, Washington, DC 20332-0001
6	Commander Naval Ordnance Station ATTN: P. L. Stang J. Birkett L. Torreyson T. C. Smith D. Brooks Tech Library Indian Head, MD 20640-5000
1	AFSC/SDOA Andrews AFB, MD 20334
3	AFRPL/DY, Stop 24 ATTN: J. Levine/DYCR R. Corley/DYC D. Williams/DYCC Edwards AFB, CA 93523-5000
1	AFFDL ATTN: TST-Lib Wright-Patterson AFB, OH 45433
1	AFRP/TSTL (Tech Library) Stop 24 Edwards AFB, CA 93523-5000
1	AFATL/DLYV Eglin AFB, FL 32542-5000
1	AFATL/DLXP Eglin AFB, FL 32542-5000
1	AFATL/DLJE Eglin AFB, FL 32542-5000
1	AFATL/DLODL ATTN: Tech Lib Eglin AFB, FL 32542-5000
1	AFWL/SUL Kirtland AFB, NM 87117
1	NASA/Lyndon B. Johnson Space Center ATTN: NHS-22, Library Section Houston, TX 77054
1	AFELM, The Rand Corporation ATTN: Library D (Required or Classified Only) 1700 Main Street Santa Monica CA 90401-3297
1	General Applied Sciences Lab ATTN: J. Erdos Merrick & Stewart Avenues Westbury Long Isld, NY 11590
2	AAI Corporation ATTN: J. Hebert J. Frankle P.O. Box 6767 Baltimore, MD 21204
1	Aerodyne Research, Inc. Bedford Research Park ATTN: V. Yousefian Bedford, MA 01730-1497
2	Calspan Corporation ATTN: C. Morphy P.O. Box 400 Buffalo, NY 14225-0400

DISTRIBUTION LIST

No. of Copies	Organization
10	Central Intelligence Agency Office of Central Reference Dissemination Branch Room GE-47 HQS Washington, DC 20505
1	General Electric Company Armament Systems Dept. ATTN: M. J. Bulman Room 1311 128 Lakeside Avenue Burlington, VT 05401-4985
1	Hercules Inc. Radford Army Ammunition Plant ATTN: J. Pierce Radford, VA 24141-0299
1	Paul Gough Associates, Inc. ATTN: P. S. Gough P.O. Box 1614 1048 South Street Portsmouth, NH 03801-1614
1	Princeton Combustion research Lab., Inc. ATTN: M. Summerfield 475 US Highway One Monmouth Junction, NJ 08852-9650
1	Battelle Memorial Institute ATTN: Tech Library 505 King Avenue Columbus, OH 43201-2693
1	Johns Hopkins University Applied Physics Laboratory Chemical Propulsion Information Agency ATTN: T. Christian Johns Hopkin oad Laurel, MD 2 -0690
1	Pennsylvania State University Dept. of Mech. Engineering ATTN: K. Kuo University Park, PA 16802-7501
2	Director Los Alamos Scientific Lab ATTN: T3, D. Butler M. Division P.O. Box 1663 Los Alamos, NM 87544

Aberdeen Proving Ground

Dir, USAMSAA
ATTN: AMXSY-D
AMXSY-MP, H. Cohen
Cdr, USATECOM
ATTN: AMSTE-TO-F
AMSTE-CM-F, L. Nealley
Cdr, CSTA
ATTN: STECS-AS-H,
R. Hendricksen
Cdr, CRDEC, AMCCOM
ATTN: SMCCR-RSP-A
SMCCR-MU
SMCCR-SPS-IL

USER EVALUATION SHEET/CHANGE OF ADDRESS

This Laboratory undertakes a continuing effort to improve the quality of the reports it publishes. Your comments/answers to the items/questions below will aid us in our efforts.

1. BRL Report Number_____ Date of Report_____

2. Date Report Received_____

3. Does this report satisfy a need? (Comment on purpose, related project, or other area of interest for which the report will be used.)_____

4. How specifically, is the report being used? (Information source, design data, procedure, source of ideas, etc.)_____

5. Has the information in this report led to any quantitative savings as far as man-hours or dollars saved, operating costs avoided or efficiencies achieved, etc? If so, please elaborate._____

6. General Comments. What do you think should be changed to improve future reports? (Indicate changes to organization, technical content, format, etc.)

CURRENT ADDRESS

Name

Organization

Address

City, State, Zip

7. If indicating a Change of Address or Address Correction, please provide the New or Correct Address in Block 6 above and the Old or Incorrect address below.

OLD ADDRESS

Name

Organization

Address

City, State, Zip

(Remove this sheet, fold as indicated, staple or tape closed, and mail.)